Eur. Phys. J. A (2026) 62:1
https://doi.org/10.1140/epja/s10050-025-01754-8

THE EUROPEAN PHYSICAL JOURNAL A

Regular Article - Experimental Physics

The study of ^{110}Cd with the $(n, n'\gamma)$ reaction revisited

P. E. Garrett[1,2,a], **J. Bangay**[1], **J. Jolie**[3], **C. S. Sumithrarachchi**[1,4], **N. Warr**[5,6], **S. W. Yates**[7]

[1] Department of Physics, University of Guelph, Guelph, Ontario N1G2W1, Canada
[2] Dept. of Physics, University of the Western Cape, P/B X17, Bellville 7535, South Africa
[3] Institut für Kernphysik, Universität zu Köln, Zülpicherstrasse 7, 50937 Köln, Germany
[4] Facility for Rare Isotope Beams, East Lansing, Michigan 48824, USA
[5] Oliver Lodge Laboratory, University of Liverpool, Liverpool L69 7ZE, UK
[6] Department of Physics and Astronomy, University of Kentucky, Kentucky 40506-0055, USA
[7] Departments of Chemistry and Physics and Astronomy, University of Kentucky, Kentucky 40506-0055, USA

Received: 6 July 2025 / Accepted: 19 November 2025

Communicated by Wolfram Korten

Abstract Data from a previous study of ^{110}Cd with the $(n, n'\gamma)$ reaction with monoenergetic neutrons have been reanalysed with the aim of identifying additional low-intensity γ-ray transitions. The data set included excitation functions measured with neutron energies between 1.94 and 3.34 MeV, and γ-ray angular distributions performed at neutron energies of 2.6, 2.9, and 3.2 MeV. A total of 162 γ rays were placed in a level scheme comprising 69 levels (of which 58 γ-ray assignments and 10 levels are newly established) up to 3.3 MeV in excitation energy. Lifetimes, or limits, were established for many levels using the Doppler-shift attenuation technique allowing for the determination of an extended set of transition rates.

1 Introduction

The stable cadmium isotopes continue to provide a testing ground for nuclear structure models. Long believed to be prime examples [1–3] of spherical vibrational motion, analysis of the extensive systematic data that are available resulted in this interpretation being called into question [4,5]. Further work [6,7] put forward the hypothesis that the mid-shell Cd nuclei possessed multiple shape coexistence – an interpretation that was also suggested for ^{106}Cd [8]. The similarity of the level schemes and the level decay properties led to the suggestion [9] that multiple shapes occur through the mid-neutron-shell Cd isotopes.

Much of the data used in the systematic evaluation of the structure of the Cd isotopes was obtained with the $(n, n'\gamma)$ reaction with accelerator-produced neutrons (see Refs. [10–20] for results on ^{110,112,114,116}Cd, respectively). The $(n, n'\gamma)$ reaction can provide extensive spectroscopic data, including level lifetimes via the Doppler-shift attenuation method [21], and comprehensive level schemes since the reaction is dominated by the compound-nucleus mechanism for low neutron energies [22]. In principle, all states in the nucleus up to an angular momentum of approximately $6\hbar$ should be populated with sufficient cross sections to be observable. As the neutron energy increases, however, the increasing complexity of the γ-ray spectrum can make the identification of decay γ rays difficult. For ^{112}Cd, it was argued in Ref. [15] that nearly all levels up to $\approx$ 3.4 MeV in excitation energy and with $I \leq 6$ were observed; at 3.4 MeV a noticeable departure from the expected exponential increase in the cumulative number of levels was noted. An examination of the results of the previous analysis [11] of the ^{110}Cd$(n, n'\gamma)$ reaction, however, suggests that a comprehensive level scheme for ^{110}Cd had not been developed to the same degree as ^{112}Cd. For example, there are many levels listed in the Nuclear Data Sheets [23] that are not listed in Ref. [11]. As well, specific excitations, such as the low-lying negative-parity states that have been observed in ^{112}Cd and ^{114}Cd with the $(n, n'\gamma)$ reaction [14,18], have also gone unreported. These facts raised one of two possible conclusions; either the $(n, n'\gamma)$ reaction was not populating all of the levels, which was considered unlikely, or the previous analysis may have been incomplete.

The study by Corminboeuf et al. [10,11] of ^{110}Cd was motivated by the desire to characterise the three-phonon states that had been assigned by Kern et al. [3,24]. As such, it was focused on the three-phonon region, at energies up to 2.5 MeV, rather than the development of a comprehensive

[a] e-mail: garrettp@uoguelph.ca (corresponding author)

Published online: 07 January 2026

level scheme. In the present work, data from the previous ^{110}Cd$(n, n'\gamma)$ reaction study have been reanalyzed. Initial results, focused on the assigned multi-phonon states and utilizing the $\gamma\gamma$ coincidences from a β-decay study of ^{110}In, were published in Ref. [25]. While only two additional transitions were placed amongst the low-lying levels, upper limits on branching ratios were determined on possible remaining transitions. These upper limits revealed that only the transition from the 6_1^+ member of the ground-state band to the 4_3^+ state of the $2p-4h$ proton intruder configuration [24,26–28] is enhanced. The decay of the intruder band head, the 0_2^+ state, has an upper limit of $B(E2; 0_2^+ \rightarrow 2_1^+) < 40$ W.u. and may be enhanced as well [25]. All other possible transitions were either not enhanced, with $B(E2)$ values on the order of a few W.u. or less, or unobserved with upper limits of at most several W.u. [25]. The results were used to conclude that the mixing between the phonon states and the intruder configuration, which had been suggested [10,28,29] to be maximal in order to reproduce the decays of the 0_2^+ and 0_3^+ levels, was, in fact, weak. This was in line with earlier suggestions by Julin et al. [30] based on the analysis of $\rho^2(E0)$ values in ^{112,114}Cd, Fahlander et al. [31] based on ^{114}Cd Coulomb-excitation results, and the possibility was raised by Casten et al. [32] based on lifetime measurements in ^{114}Cd.

Following the initial result of Ref. [25] exploring the intruder-phonon mixing, more extensive analysis combining the $(n, n'\gamma)$ data and that from the ^{110}In decay were used to establish a series of rotational-like bands in ^{110}Cd that were interpreted in a multiple shape-coexistence scenario [6,7]. This interpretation was a radical departure from the spherical multi-phonon vibrational interpretation that has been questioned not only in the Cd isotopes, but in many of the U(5) symmetry candidates [3] in the region [33]. However, the vibrational interpretation was revived invoking a partial-dynamical symmetry [34] that preserves the U(5) symmetry for some of the levels, while strongly perturbing it for others [35,36]. This approach reconciled the experimentally observed violation of the normal phonon selection rules for γ-ray decays with the vibrational interpretation by, in effect, exchanging the positions of the 0^+ and 2^+ two and three phonon states with the three and four phonon states, respectively.

The suggestion of an alternative interpretation of the structure of ^{110}Cd as possessing multiple shape coexistence has spurred extensive investigations using Coulomb excitation which has included the use of ^{14}N, ^{32}S, ^{60}Ni, and ^{208}Pb as binary reaction partners. The first results [37,38] of the campaign using beams of ^{14}N and ^{32}S determined the $\langle Q^2 \rangle$ and $\langle Q^3 \cos 3\delta \rangle$ invariant quantities [39,40] for the ground state, leading to $\beta(0_1^+) \approx 0.17$ and $\gamma \approx 23°$, i.e., a triaxial shape. For the 0_2^+ state, the $\langle Q^2 \rangle$ was determined leading to $\beta(0_2^+) \approx 0.19$. These results indicate that the overall deformation of the ground state and the intruder band head are not significantly different, but the shape of the intruder 0^+ state remains unknown. The analysis of the Coulomb-excitation data is greatly facilitated by including complementary data such as measured transition branching ratios, multipole mixing ratios, and level lifetimes. Since the use of high-Z partners can lead to the population of a myriad of levels to both high spin and high excitation energy, the development of a comprehensive level scheme is paramount, motivating the current reanalysis which has resulted in a total of 162 transitions placed in the level scheme of ^{110}Cd, with 10 new levels observed and a refinement of spin-parity assignments for several others. The details of the reanalysis and the results are presented in Sect. 2, with an interpretation of the levels in Sect. 3.

2 Experimental details and results

As the data presented herein arises from the same experiment as outlined by Corminboeuf et al. [10,11], and partial results of the reanalysis were published in Refs. [6,7,25], the experimental details will not be repeated at length here. Rather, we concentrate on the differences in the analysis.

In any particular experiment, a single HPGe detector equipped with an annular BGO Compton-suppression shield was used. The HPGe detectors had either 52% or 57% relative efficiency, and a full width at half maximum between 1.9 and 2.0 keV at 1332 keV, depending on the experiment. The amplified detector signals were processed by a 16k-channel AD114 Ortec amplitude-to-digital converter. The gain on the amplifier was adjusted to achieve the greatest possible dispersion (i.e., channels/keV) while providing full coverage of the possible γ rays emitted in the measurements. The non-linearity of the detector plus data acquisition system was determined through the use of radioactive sources of ^{152}Eu, ^{226}Ra and ^{56}Co. For the angular-distribution measurements, the in-beam data were collected simultaneously with ^{60}Co and ^{24}Na sources that, together with the well-known 657.8 keV γ-ray transition in ^{110}Cd, provided the absolute energy calibration following corrections for the system non-linearity. The simultaneous collection of radioactive-source data also enabled a sensitive monitoring of potential gain drifts.

For the lifetime determinations, the γ-ray energies were fitted with

$$E_\gamma(\theta) = E_\gamma^o [1 + \beta F(\tau) \cos\theta] \quad (1)$$

where $E_\gamma(\theta)$ is the observed γ-ray energy at an angle θ with respect to the forward recoil direction, taken to be the beam direction, E_γ^o is the unshifted γ-ray energy, and $\beta = v/c$ is the recoil velocity in the center-of-mass frame. By examining the energy of a γ ray as a function of angle, the attenuation

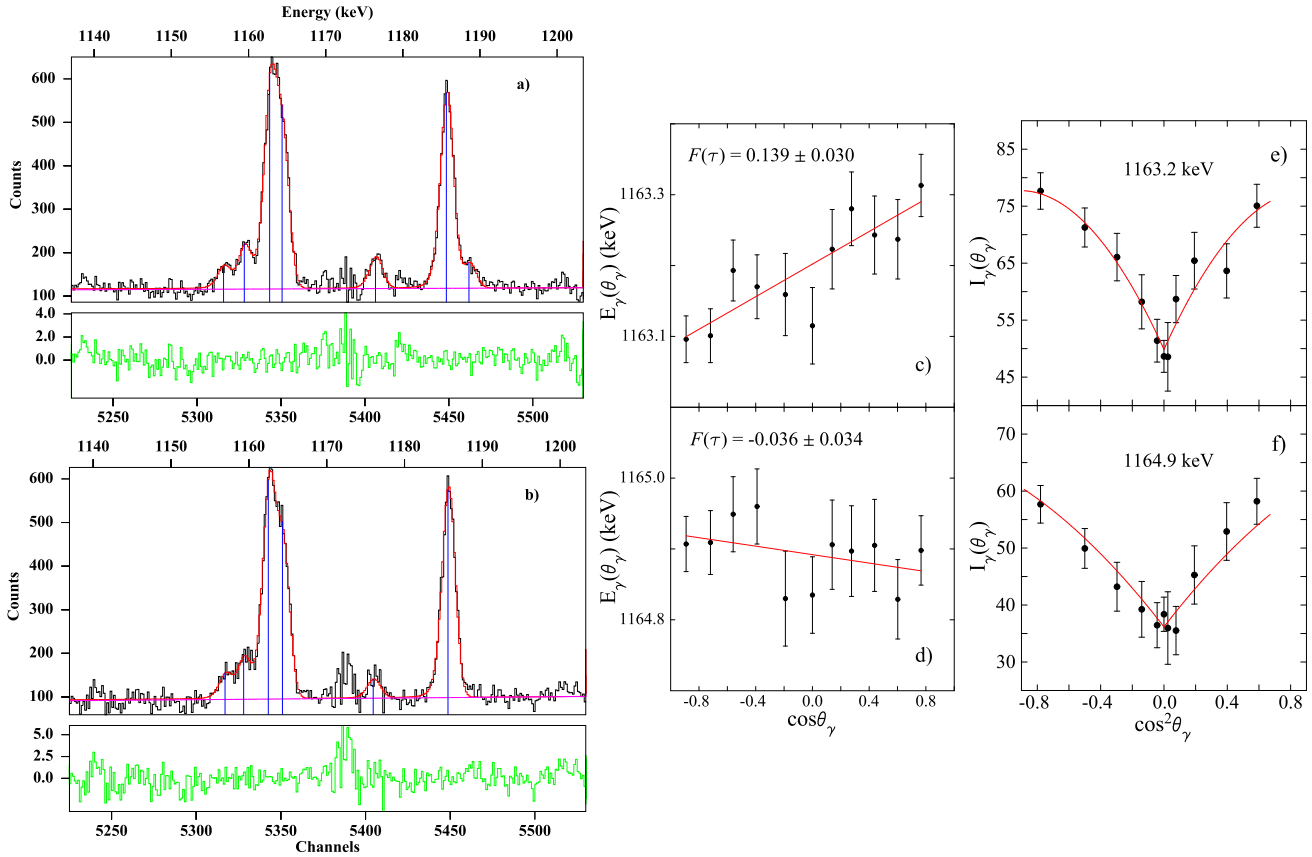

Fig. 1 Examples of fits of unresolved γ-ray peaks. Panel a) displays the region near the 1163.2-keV γ ray that is unresolved from the 1164.9 keV γ ray. The data were obtained for a neutron bombarding energy of 2.9 MeV and with the detector positioned at an angle of 40° with respect to the proton beam axis. The black histogram are the data that result from a subtraction of the out-of-beam background from the data taken coincident with the proton beam pulse. The fluctuation observed near 1173 keV is the net result of the subtraction for a very large peak due to the 1173.2-keV γ ray from a ^{60}Co source. The red histogram is the result of a fit of the spectrum, with the peak centroids indicated by blue markers, and the linear background given in magenta. The histogram in green is the residual defined as the difference in the observed data and fit histograms divided by the square root of the number of counts of the black histogram. Panel b) shows the resulting spectrum collected at $\theta = 153°$. The small peak at 1189 keV observed in the $\theta = 40°$ spectrum (a) originates from an angle-dependent, prompt, background line. Panel c) and d) display the measured peak energies for the 1163.2-keV γ ray and the 1164.9-keV γ ray, respectively. The $F(\tau)$ values that result from the fit using Eq. 1 (red line) are given. The data for the 1164.9-keV γ ray has a $F(\tau)$ value consistent with 0, with a maximum difference in the measured energies of 131 eV and standard deviation of 42 eV. The average uncertainty on the measured energy is 55 eV. Panels e) and f) show the extracted angular distributions for the two γ rays, and the red curves are the fit to the data using Eq. 2. The data are plotted versus $\cos^2\theta_\gamma$ where the negative sign indicates angles greater than 90°

factor $F(\tau)$ can be obtained, and the lifetime τ of the state can be determined [21] by a comparison with the $F(\tau)$ value calculated using the Winterbon formalism [41]. The fit also yields the most accurate measure of the γ-ray energy, E_γ^o.

There are two main areas of improvement in the analysis of the experimental data. Firstly, care was taken to ensure consistency of fits of observed peaks across the many spectra obtained from the experiment. This included the fixing of the peak-shape parameters (the model of the peak shape used is that of Kern et al. [42]). Whenever possible, identical sets of parameters were used for fitting the spectra that arose from a particular experimental run; in only a few cases did the width as a function of channel number of the Gaussian used to fit the peaks need to be adjusted, and these adjustments were very minor. Whenever possible, the number and approximate positions of the peaks in a fit region of the spectrum were kept constant from angle to angle (for the angular distributions). Figure 1 displays a small portion of the observed γ-ray spectra taken in the angular distribution measurement at $E_n = 2.9$ MeV. We focus on the fits for an unresolved pair of γ rays at 1163.2-keV and 1164.9 keV that aptly display the ability to extract reliable data. The peak-shape parameters, that were fixed by a global fit to data from well-resolved peaks across the full range of the spectrum, reproduce the shape of the peak at 1186.2 keV extremely well, with panel a) displaying the data taken at a detector angle of $\theta = 40°$,

and panel b) those at $\theta = 153°$. The resulting γ-ray energies extracted from the peak centroids are shown in panels c) for the 1163.2-keV peak and d) for the 1164.9-keV peak. The $F(\tau)$ value for the 1164.9-keV γ-ray peak has a small negative value consistent with zero, with the maximum difference in the measured energy of 0.131 keV corresponding to approximately 0.6 channels. The resulting angular distributions are shown in panels e) and f) and show that despite the unresolved nature of this particular pair of γ rays, individual angular distributions can still be extracted.

In order to test of the accuracy of both the γ-ray centroid shift measurements, as well as the absolute γ-ray energy determinations, the 1173.228(3)-keV [43] γ-ray line from ^{60}Co was not used in the calibrations for the angular distribution measurements. For the three angular distributions using 2.6 MeV, 2.9 MeV, and 3.2 MeV neutrons, energies E_γ^o of 1173.246(6) keV, 1173.201(3) keV, and 1173.235(5) keV were determined with $F(\tau)$ values of $-0.008(11)$, $-0.004(6)$, and 0.014(10), respectively. The uncertainties on the energies result from the fit performed using Eq. 1 with uncertainties of the γ-ray energies for each angle determined with a full covariance matrix calculation. For intense, well-resolved γ-ray peaks, very similar spreads in the absolute energies were observed and we thus recommend that a 20 eV systematic uncertainty be applied to the γ-ray energies listed in Table 1. The $F(\tau)$ values extracted for the 1173.2-keV γ-ray peak give an indication of the limitation of the method in the present case. For small $F(\tau)$ values, and hence long lifetimes, further experiments should be performed to confirm or refine the present results.

New peaks in the observed γ-ray spectra had to be introduced, by necessity, with angle-dependent backgrounds or with the increasing neutron energy. For the latter, once a peak was positively identified and introduced they were not removed in the spectra obtained at higher neutron energies. This became important as the complexity of the spectra increased and the probability of peaks becoming members of unresolved multiplets also increased.

The second main area of improvement in the data analysis was in the identification of weak peaks in the spectra. A large number of very small peaks that were overlooked in the previous analysis were included in the present work. The identification of these low-intensity γ rays enabled assignments of additional transitions from levels, thereby increasing the confidence of their placement and the existence of the levels. Figure 2 displays portions of the spectra collected at neutron bombarding energies of 2.14 MeV (upper panel) and 2.94 MeV (lower panel) during the excitation-function measurement. The red lines indicate newly-placed γ rays that were not reported in Refs. [10,11]. As in the previous work [10,11], a serious weakness is the lack of $\gamma\gamma$ coincidence data. Weak transitions from low-lying levels could be verified using $\gamma\gamma$ coincidence data from the β decay of ^{110}In, as reported in Ref. [25]. Since that decay was dominated by the ^{110}In 7^+ ground state, its sensitivity to low-spin, highly non-yrast states was compromised and above approximately 2.5 MeV there is a decreasing overlap between levels observed in the present $(n, n'\gamma)$ reaction data and the β-decay data. The sole reliance on excitation function data and Ritz combinations can thus lead to uncertainties in the placements of transitions, particularly for transitions that do not feed the 0_1^+ or 2_1^+ states.[1] For this reason, the present work reports in Table 1 on all levels and placements of transitions below 3 MeV. Above this excitation energy primarily only the γ-ray decays to the ground state and first 2^+ state are reported and an increasing number of observed transitions remain unplaced, which are reported together with their neutron threshold energy in Table 2.

The results listed in Table 1 report the $F(\tau)$ and lifetime values extracted from the data obtained with the lowest neutron bombarding energy for which the transitions are observed with sufficient intensity. For the majority of states for which lifetimes are reported, the feeding from states at higher excitation energy is negligible. However, feeding may affect the lifetimes extracted for levels at low excitation energy even in the case of data obtained at 2.6 MeV. The only case, discussed below, where we ascertain that feeding may have a significant impact on the extracted lifetime is for the 1475-keV 2_2^+ level.

Lifetimes deduced in the present analysis are, in general, in good agreement with those of the previous analysis [11] with the largest deviation occurring for the 2220-keV 4_2^+ level that has a lifetime of 1510^{+1140}_{-460} fs from the present analysis compared with 970^{+430}_{-230} fs [10,11]. The inconsistency in the lifetime values is due to differences in the fits for the 677.6-keV transition with the inclusion of a small peak due to a background line at 679.7-keV; the present measurement is $F(\tau) = 0.024 \pm 0.010$, whereas Corminboeuf et al. [11] obtained $F(\tau) = 0.040 \pm 0.014$. Other lifetimes compare very favourably, although the uncertainties have been reduced considerably for most levels. For example, the fits for the γ rays originating from the 1783-keV level yield an identical result $\tau = 1160$ fs, but the uncertainties are reduced from $(+490, -270)$ [11] to $(+170, -140)$ fs. Examples of the presently extracted Doppler shifts are shown in Fig. 3. For the 1473-keV and 1731-keV 0^+ levels, limits on lifetimes greater than 1.8 ps and 2 ps, respectively, are obtained. For the 2480-keV 6^+ level, the data are inconsistent between the 2.9-MeV and 3.2-MeV angular distributions with the former

[1] The results of the analysis of the excitation-function data are very sensitive to the presence of unresolved γ-ray peaks through the examination of the peak centroid and branching ratio as a function of bombarding neutron energy, as well as sudden changes in the smooth evolution of the γ-ray yield. A constant measured γ-ray energy and consistent branching ratio, but a sudden increase in the yield, may reflect feeding of the level from a higher-lying state.

Table 1 Results for ^{110}Cd from the $(n, n'\gamma)$ reaction. The first two columns list the recent evaluated level scheme [23]. Uncertainties are listed in parentheses. The γ-ray energy uncertainties are statistical only, and do not include an estimated 20 eV systematic uncertainty (see text for details), but this has been taken into account for the determination of the level energies. The I_γ values are the relative intensity of the observed γ rays for each level, normalized to 1.0. For some transitions, the angular distribution analysis leads to ambiguities in the value of the mixing ratio δ; the second value listed has a larger χ^2 value, but cannot be excluded. The $F(\tau)$ value listed for a level is the weighted average of the values observed for individual γ rays from the level. The last column indicates if the level (L) or the γ-ray placement (γ) is new to the present study; a n.o. listing indicates that the level was not observed and concluded not to exist. Levels listed under NDS but without a n.o. entry are unobserved in the present study, but their non-existence cannot be concluded

NDS E_i (keV)	NDS I_i^π	E_i (keV)	I_i^π	E_γ (keV)	E_f (keV)	I_f^π	I_γ	δ	$F(\tau)$	τ (fs)	New level or γ
657.7623(11)	2^+	657.7623(11)[a]	2_1^+	657.7600(11)[a]	0.0	0_1^+	1.0				
1473.07(3)	0^+	1473.088(21)	0_2^+	815.323(3)	657.8	2_1^+	1.0		0.011(9)	> 1800	
1475.7900(14)	2^+	1475.806(11)	2_2^+	818.034(3)	657.8	2_1^+	0.643(10)[b]	$-2.17^{+0.35}_{-0.36}$	0.019(4)	1950^{+500}_{-330}	
				1475.799(8)	0.0	0_1^+	0.357(10)[b]			1600^{+700}_{-400} [c]	
1542.4441(14)	4^+	1542.444(16)	4_1^+	884.688(3)	657.8	2_1^+	1.0				
1731.31(3)	0^+	1731.314(19)	0_3^+	255.547(15)	1475.8	2_2^+	0.143(8)[b]		$-0.003(7)$	> 2000	
				1073.549(7)	657.8	2_1^+	0.857(8)[b]				
1783.496(15)	2^+	1783.559(14)	2_3^+	307.8[d]	1475.8	2_2^+	< 0.0009[b]		0.032(4)	1160^{+170}_{-140}	
				310.515(38)	1473.1	0_2^+	0.0037(4)[b]				
				1125.789(5)	657.8	2_1^+	0.772(8)[b]	$0.186^{+0.038}_{-0.028}$			
								$1.52^{+0.12}_{-0.09}$			
				1783.583(14)	0.0	0_1^+	0.224(6)[b]				
1809.48(9)	4^+										n.o.
2078.548(11)	3^-	2078.875(31)	3_1^-	295.3[d]	1783.6	2_3^+	0.0100(7)[e]		0.047(5)	750^{+100}_{-80}	
				603.067(5)	1475.8	2_2^+	0.135(5)[e]	$0.036^{+0.016}_{-0.063}$		630^{+90}_{-80} [c]	
				1421.1[d]	657.8	2_1^+	0.855(5)[e]				
2078.80(5)	0^+	2078.892(21)	0_4^+	295.3[d]	1783.6	2_3^+	0.791(21)[b]				
				603.1[d]	1475.8	2_2^+	< 0.18[b]				
				1421.1[d]	657.8	2_1^+	0.209(21)[b]				
2162.8015(15)	3^+	2162.822(19)	3_1^+	379.2[d]	1783.6	2_3^+	< 0.003[b]		0.022(6)	1640^{+700}_{-380}	
				620.300(20)	1542.5	4_1^+	0.117(4)[b]	$-0.36^{+0.04}_{-0.05}$			
								$-1.93^{+0.24}_{-0.28}$			
				687.004(4)	1475.8	2_2^+	0.287(9)[b]	$-1.79(10)$			
				1505.046(11)	657.8	2_1^+	0.596(10)[b]	$-1.47^{+0.10}_{-0.11}$			
2184(2)	(1^-)										n.o.
2198(2)	$2^+, 3^+$										n.o.
2220.0683(14)	4^+	2220.106(19)	4_2^+	436.5[d]	1783.6	2_3^+	< 0.0003[b]		0.024(10)	1510^{+1140}_{-460}	
				677.623(4)	1542.5	4_1^+	0.630(9)[b]	$-0.41(3)$			
				744.307(10)	1475.8	2_2^+	0.293(9)[b]				
				1562.324(52)	657.8	2_1^+	0.076(3)[b]				
2250.554(11)	4^+	2250.578(23)	4_3^+	466.997(16)	1783.6	2_3^+	0.104(4)[b]		0.033(9)	1080^{+450}_{-250}	
				708.122(4)	1542.5	4_1^+	0.813(6)[b]	$0.131^{+0.044}_{-0.036}$			
				774.91(12)	1475.8	2_2^+	0.0160(7)[b]				
				1592.824(58)	657.8	2_1^+	0.067(3)[b]				
2287.63(11)	2^+	2287.485(30)	2_4^+	1629.711(10)	657.8	2_1^+	1	$2.22^{+0.19}_{-0.18}$	0.085(5)	395^{+30}_{-24}	
								$0.02^{+0.027}_{-0.036}$			
2331.92(4)	$(0)^+$	2331.920(29)	0_5^+	548.275(51)	1783.6	2_3^+	0.0335(20)		0.013(9)	2800^{+5300}_{-1100}	
				856.074(55)	1475.8	2_2^+	0.0425(25)				γ
				1674.182(15)	657.8	2_1^+	0.924(3)				

Table 1 continued

NDS E_i (keV)	NDS I_i^π	E_i (keV)	I_i^π	E_γ (keV)	E_f (keV)	I_f^π	I_γ	δ	$F(\tau)$	τ (fs)	New level or γ
2355.792(19)	2^+	2355.753(25)	2_5^+	572.2[d]	1783.6	2_3^+	< 0.006[b]		0.070(6)	484^{+47}_{-38}	
				624.364(36)	1731.3	0_3^+	0.0416(11)[b]				
				813.3[d]	1542.5	4_1^+	< 0.03[b]				
				880.0[d]	1475.8	2_2^+	0.0217(13)[b]	$0.66^{+0.51}_{-0.34}$			
				882.7[d]	1473.1	0_2^+	< 0.017[b]				
				1698.029(12)	657.8	2_1^+	0.9367(16)[b]	2.7(3)			
								$-0.050^{+0.034}_{-0.045}$			
2365(2)	2^+										n.o.
2377(2)	4^+										n.o.
2381(2)											n.o.
2385(2)	(2^+)										n.o.
2405(2)	$(0^+, 2^-)$										n.o.
2433.248(25)	3^+	2433.227(24)	3_2^+	270.379(53)	2162.8	3_1^+	0.051(2)	$2.4^{+5.5}_{-1.2}$	0.010(9)	> 1900	γ
				354.251(58)	2078.9	3_1^-	0.012(2)				γ
				890.723(34)	1542.5	4_1^+	0.124(3)	$-0.53^{+0.23}_{-1.22}$			
				957.439(8)	1475.8	2_2^+	0.544(4)	$-1.75^{+0.12}_{-0.14}$			
				1775.498(44)	657.8	2_1^+	0.269(4)	$-4.6^{+1.1}_{-1.7}$			
2477.41(5)	2^+	2477.405(18)	2_6^+	314.594(78)	2162.8	3_1^+	0.060(1)	$-0.30^{+0.09}_{-0.11}$	0.009(8)	> 2000	γ
								$-1.99^{+0.42}_{-0.53}$			
				398.497(7)	2078.9	3_1^{-f}	0.098(2)				γ
				746.140(12)	1731.3	0_3^+	0.138(2)				
				1001.545(37)	1475.8	2_2^+	0.318(2)	$-0.157^{+0.031}_{-0.034}$			
								$-4.0^{+0.8}_{-0.6}$			
				1004.55(14)	1473.1	0_2^+	0.050(16)				γ
				1819.646(25)	657.8	2_1^+	0.053(1)	$3.82^{+0.65}_{-0.38}$			
				2477.366(16)	0.0	0_1^+	0.284(3)				
2479.9339(25)	6^+	2479.787(43)	6_1^+	229.4[d]	2250.6	4_3^+	0.00051(3)[b]				
				259.9[d]	2220.1	4_2^+	< 0.0001[b]				
				937.511(44)	1542.5	4_1^+	0.99949(3)[b]				
2481.606(20)	(2^+)	2481.641(31)	3_2^-	402.626(39)	2078.9	3_1^-	0.123(2)	$0.23^{+0.15}_{-0.10}$	0.060(8)	566^{+84}_{-70}	
				697.973(10)	1783.6	2_3^+	0.121(3)	0.016(47)			
				1005.749(23)	1476.3	2_2^+	0.249(2)	0.030(33)			
				1823.759(7)	657.8	2_1^+	0.508(3)	$0.009^{+0.022}_{-0.025}$			
2539.691(6)	5^-	2539.641(31)	5_1^-	460.715(59)	2078.9	3_1^-	0.033(4)		0.023(17)	1550^{+5090}_{-680}	
				997.196(6)	1542.5	4_1^+	0.966(4)	0.000(16)			
2561.284(9)	4^+	2561.255(22)	4_4^+	1018.801(21)	1542.5	4_1^+	0.131(4)	$4.2^{+4.8}_{-1.4}$	0.026(12)	1330^{+1180}_{-430}	
								$-0.57^{+0.17}_{-0.26}$			
				1085.486(6)	1475.8	2_2^+	0.704(4)				
				1903.383(25)	657.8	2_1^+	0.165(3)				
2566.47(6)	$(2^-, 3)$	2566.468(18)	3_3^+	782.937(14)	1783.6	2_3^+	0.097(1)	$-25^{+12}_{-\infty}$	0.044(8)	771^{+176}_{-122}	
								0.15(4)			
				1090.654(7)	1475.8	2_2^+	0.269(2)	0.33(3)			

Table 1 continued

NDS E_i (keV)	NDS I_i^π	E_i (keV)	I_i^π	E_γ (keV)	E_f (keV)	I_f^π	I_γ	δ	$F(\tau)$	τ (fs)	New level or γ
				1908.665(7)	657.8	2_1^+	0.634(2)	0.20(2)			
2633.20(9)	2^+	2633.050(22)	2_7^+	554.162(27)	2078.9	3_1^- [f]	0.042(2)		0.157(8)	194^{+11}_{-10}	γ
				1157.274(56)	1475.8	2_2^+	0.031(2)	$3.7^{+28}_{-1.9}$			
								$-0.14^{+0.24}_{-0.26}$			
				1159.983(35)	1473.1	0_2^+	0.048(2)				γ
				1975.250(7)	657.8	2_1^+	0.870(3)	$0.272^{+0.036}_{-0.048}$			
								$1.26^{+0.11}_{-0.13}$			
				2633.1(1)	0.0	0_1^+	0.009(3)				γ
2649.95(6)	1^-	2649.743(32)	1_1^-	1176.590(25)	1473.1	0_2^+	0.055(3)		0.512(9)	36(1)	
				2649.763(24)	0.0	0_1^+	0.945(3)				
2659.866(7)	5^-	2659.861(40)	5_2^-	409.402(87)	2250.6	4_3^+	0.104(15)	$-0.02^{+0.15}_{-0.14}$	0.032(52)	> 384	
				1117.399(20)	1542.5	4_1^+	0.896(15)	$-0.003(31)$			
2662.13(10)	0^+	2662.010(18)	$0_6^+/3_4^+$	184.686(33)	2477.4	2_6^+					γ
				306.324(29)	2355.8	2_5^+					γ
				441.892(9)	2220.1	4_2^+		$-0.009^{+0.025}_{-0.038}$			γ
								$-6.9^{+1.1}_{-2.2}$			
				878.497(41)	1783.6	2_3^+					γ
				1119.7(1)	1542.5	4_1^+		$-0.05(16)$			γ
								$-5.8^{+2.9}_{-58}$			
				1186.156(9)	1475.8	2_2^+					
				2004.205(15)	657.8	2_1^+					
2705.669(10)	(4^+)	2705.650(38)	4_5^+	1163.199(15)	1542.5	4_1^+	1.0	$1.18^{+0.20}_{-0.18}$	0.139(30)	221^{+68}_{-44}	
								$-0.04(7)$			
2707.397(8)	(4^+)	2707.389(26)	(4_1^-)	544.589(13)	2162.8	3_1^+	0.296(6)	$0.014^{+0.033}_{-0.030}$ [g]	$-0.036(34)$	> 1000	
				628.552(38)	2078.9	3_1^-	0.142(6)	0.19(7) [g]			γ
								$13^{+\infty}_{-7}$ [g]			
				1164.890(17)	1542.5	4_1^+	0.563(8)	$0.02^{+0.12}_{-0.10}$ [g]			
2758.25(8)	$2^-, (1, 2, 3)^+$	2758.219(39)	2_1^-	974.794(39)	1783.6	2_3^+	0.085(5)	$0.03^{+0.24}_{-0.21}$	0.119(22)	262^{+67}_{-46}	γ
				1282.384(14)	1475.8	2_2^+	0.670(6)	$-0.06^{+0.06}_{-0.05}$			
				2100.376(32)	657.8	2_1^+	0.245(6)	$-0.01(9)$			
2787.49(4)	2^+	2787.251(36)	2_8^+	2129.467(17)	657.8	2_1^+	0.953(10)	$0.20^{+0.07}_{-0.06}$	0.491(18)	38(3)	
								$1.46^{+0.23}_{-0.21}$			
				2787.4(4)	0.0	0_1^+	0.046(10)				
2793.441(7)	(4^+)	2793.480(34)	4_6^+	573.323(34)	2220.1	4_3^+	0.342(39)	$-0.9^{+0.3}_{-4.3}$			
				630.597(56)	2162.8	3_1^+	0.309(50)	$-1.5^{+1.1}_{-1.1}$			
								$-0.7^{+0.3}_{-1.8}$			
				714.5 [d]	2079.0	3_1^-	[h]				
				1251.078(25)	1542.5	4_1^+	0.349(36)	$-0.11^{+0.21}_{-0.20}$			
								$1.9^{+1.8}_{-0.8}$			
2813(3)											n.o.
2834(3)	$3^+, 4^+$										n.o.
2842.682(10)	(5^-)	2842.662(42)	5_3^-	1300.209(20)	1542.5	4_1^+	1.0	$-0.036^{+0.052}_{-0.059}$	$-0.003(70)$	> 500	
2869.114(23)	$1^+, 2^+$	2869.272(40)	2_9^+	1085.6[d]	1783.6	2_3^+	[h]		0.404(26)	55^{+6}_{-5}	

Table 1 continued

NDS E_i (keV)	NDS I_i^π	E_i (keV)	I_i^π	E_γ (keV)	E_f (keV)	I_f^π	I_γ	δ	$F(\tau)$	τ (fs)	New level or γ
				1393.74(10)	1475.8	2_2^+	0.041(5)	0.040(5)			
				1396.0[d]	1473.1	0_2^+	0.032(4)				γ
				2211.463(24)	657.8	2_1^+	0.912(30)	$0.12^{+0.12}_{-0.10}$			
								$1.82^{+0.60}_{-0.44}$			
				2869.04(22)	0.0	0_1^+	0.015(2)				
2876.812(10)	6^+	2876.51(30)	6_2^+	1334.06(22)	1542.5	4_1^+	1.0				
2895.948(13)	6^-										
		2916.337(49)	(3^+)	837.50(7)	2078.9	3_1^-	0.112(24)			> 250	L/γ
				1132.795(55)	1783.6	2_3^+	0.256(12)	$-3.8^{+1.0}_{-1.9}$			γ
								$-0.15^{+0.09}_{-0.12}$			
				1373.825(70)	1542.5	4_1^+	0.246(14)	$-0.16^{+0.26}_{-0.37}$			γ
								$-3.1^{+1.8}_{-12.8}$			
				1440.48(14)	1475.8	2_2^+	0.118(43)				γ
				2258.575(59)	657.8	2_1^+	0.249(12)	$0.03^{+0.21}_{-0.24}$			
								-11^{+8}_{-18}			
2917.60(7)	$2^+,3,4^+$	2917.899(60)	(4^+)	667.33(7)	2250.6	4_3^+	0.32(6)				γ
				1375.544(49)	1542.5	4_1^+	0.68(6)				γ
2926.7474(16)	5^+	2926.809(47)	5_1^+	446.8[d]	2479.9	6_1^+	0.0741(8)[i]		0.129(83)	240^{+500}_{-110}	
				706.7[d]	2220.1	4_2^+	0.2275(20)[i]				
				763.924(31)	2162.8	3_1^+	0.3337(25)[j]				
				1384.557(65)	1542.5	4_1^+	0.3647(26)[j]				
2938(3)	2^+										n.o.
		2960.379(67)	3_3^-	420.78(6)	2539.7	5_1^-	0.130(13)				L/γ
				881.5[d]	2078.9	3_1^-	0.590(22)				γ
				1176.7[d]	1783.6	2_3^+	[h]				γ
				1417.92(9)	1542.5	4_1^+	0.280(20)				γ
2975.24(4)	$1^+,2^+$	2975.267(68)	(2^+)	896.4[d]	2078.9	$0_4^+/3_1^-$	0.124(32)				
				2317.469(48)	657.8	2_1^+	0.822(34)	$0.06^{+0.25}_{-0.20}$			
								$2.1^{+1.8}_{-0.9}$			
				2975.31(16)	0.0	0_1^+	0.056(12)				
2984.48(6)	(5^-)	2984.35(10)		1441.89(7)	1542.5	4_1^+	1.0				
2984.46(14)	$2^+,3^+$	2984.578(32)	(2^+)	503.002(40)	2481.5	3_2^-	0.333(8)				γ
				905.682(22)	2078.9	3_1^-	0.424(9)				
				2326.89(9)	657.8	2_1^+	0.243(6)				
2991(3)	(5^-)										
2993.63(17)	(0^+)										n.o.
2994.07(8)	$(3^+,4^+)$	2993.88(10)	$3,4^+$	1209.86(13)	1783.6	2_3^+	0.265(9)				
				1451.63(8)	1542.5	4_1^+	0.606(11)				
				1518.15(9)	1475.8	2_2^+	0.129(9)				
3008.4(7)?	$1,2^+$										n.o.
		3008.517(88)	(5^+)	788.39(10)	2220.1	4_2^+	0.317(45)				
				845.70(8)	2162.8	3_1^+	0.64(9)				
				1466.0[b]	1542.5	4_1^+	0.18(3)				
3021(3)	(1^-)										n.o.

Table 1 continued

NDS E_i (keV)	NDS I_i^π	E_i (keV)	I_i^π	E_γ (keV)	E_f (keV)	I_f^π	I_γ	δ	$F(\tau)$	τ (fs)	New level or γ
3040(3)	0^+	3042.92(9)	0^+	1566.92(7)[k]	1475.8	2_2^+	0.35(7)				
				2385.94(14)[k]	657.8	2_1^+	0.65(7)				
3042.86(8)	1^+	3043.39(20)	1^+	1569.88(40)	1473.1	0_2^+	0.088(20)				γ
				3043.4(5)	0.0	0_1^+	0.912(20)				
		3049.6(5)	0–4	2391.84(39)	657.8	2_1^+	1.0				L/γ
3052(3)	2^+										n.o.
		3055.690(69)	$3,4^+$	1271.99(11)	1783.6	2_3^+	0.113(19)				L/γ
				1513.53(12)	1542.5	4_1^+	0.292(9)				γ
				1579.883(65)	1475.8	2_2^+	0.549(25)				γ
				2397.59(17)	657.8	2_1^+	0.064(6)				γ
3064.712(13)	6^+	3064.27(26)	6_3^+	844.16(19)	2220.1	4_2^+	1.0				
3073(3)	$(1^+,2^+)$	3076.33(20)	$1,2^+$	(1603.23(14))[l]	1473.1	0_2^+	1.0				(γ)
3078.381(23)	$1^{(+)}$	3077.450(74)	1	1601.38(11)	1475.8	2_2^+	0.183(10)				
				2419.71(6)	657.8	2_1^+	0.443(17)				
				3077.8(5)	0.0	0_1^+	0.374(21)				
3101.88(3)	2^+	3101.828(56)		1023.071(62)	2078.9	$0_4^+/3_1^-$	0.200(18)				
				1626.15(9)	1475.8	2_2^+	0.229(23)				
				2443.846(59)	657.8	2_1^+	0.569(41)				
3106(3)	$3^+, 4^+$	3108.619(52)	$3,4^+$	858.13(9)	2250.6	4_3^+	0.125(9)				γ
				888.40(7)	2220.1	4_2^+	0.274(11)				γ
				945.780(48)	2162.8	3_1^+	0.164(4)				γ
				1030.015(38)	2078.9	3_1^-	0.189(18)				γ
				1325.37(14)	1783.6	2_3^+	0.044(7)				γ
				1632.78(8)	1475.8	2_2^+	0.139(13)				γ
				2450.30(12)	657.8	2_1^+	0.063(7)				γ
3118(3)	2^+										n.o.
3121.62(3)	6^+										
3128.41(7)	$1^+, 2^+$	3128.277(82)	(2^+)	1049.32(9)	2078.9	$0_4^+/3_1^-$	0.311(50)				γ
				1344.82(11)	1783.6	2_3^+	0.211(70)				
				(1397.0)[l]	1731.3	0_3^+					(γ)
				1652.41(12)	1475.8	2_2^+	0.215(28)				
				3128.6(5)	0.0	0_1^+	0.261(13)				
3135.18(7)	$2^+, 3^+$										n.o.
3142(2)	2^+–4^+	3143.66(23)		1360.09(17)	1783.6	2_3^+	1.0				γ
		3147.393(80)	(4^+)	927.16(13)	2220.1	4_2^+	0.151(17)				L/γ
				1068.23(18)	2078.9	3_1^-	0.107(15)				γ
				1363.894(61)	1783.6	2_3^+	0.415(18)				γ
				1671.1(4)	1475.8	2_2^+	0.076(16)				γ
				2489.28(19)	657.8	2_1^+	0.251(14)				γ
3148(3)	0^+	3151.47(16)		2493.67(11)	657.8	2_1^+	1.0				γ
		3163.8(4)		2506.0(3)	657.8	2_1^+	1.0				L/γ
		3166.25(26)		2508.45(19)	657.8	2_1^+	1.0				L/γ
3171.19(20)	2^+–4^+	3170.44(14)		2512.643(81)	657.8	2_1^+	1.0				
3183(3)	(4^+)										
3184.53(3)	$5^-, 6^-$										

Table 1 continued

NDS E_i (keV)	NDS I_i^π	E_i (keV)	I_i^π	E_γ (keV)	E_f (keV)	I_f^π	I_γ	δ	$F(\tau)$	τ (fs)	New level or γ
3193.40(4)	(3^+)	3193.39(12)		1410.08(21)	1783.6	2_3^+	0.139(22)				
				1717.37(23)	1475.8	2_2^+	0.147(19)				
				2535.58(10)	657.8	2_1^+	0.714(23)				
3199(3)	(2^-)										
3203(3)		3203.28(25)		2545.48(18)	657.8	2_1^+	1.0				γ
		3206.5(8)		2548.7(5)	657.8	2_1^+	1.0				L/γ
3208.69(7)	$2^+, 3^+$										
3251(3)	3^-										
3256.49(14)	1^+–3^+	3256.41(21)	2^+–4^+	1714.31(22)	1542.5	4_1^+	0.239(28)				γ
				2598.28(21)	657.8	2_1^+	0.761(28)				
3262(3)	1^+–3^+										
		3266.49(52)		2608.69(38)	657.8	2_1^+	1.0				L/γ
3277.86(14)	(1^+)	3277.16(25)		2619.36(18)	657.8	2_1^+	1.0				
		3281.1(7)		3281.0(5)	0.0	0_1^+	1.0				L γ
3298.13(20)	1^-	3298.2(8)		3298.1(6)	0.0	0_1^+	1.0				

[a] Value from Ref. [23] and used for calibration
[b] Branching ratio taken from Ref. [25]
[c] Lifetime calculated with a correction assuming $\tau > 10$ ps for the 0_4^+ state
[d] Value obtained from difference in level energies
[e] Branching ratio could not be determined in present measurement; value obtained from β decay
[f] Placement feeding the 3_1^- level assumed; placement feeding the 0_4^+ level cannot be conclusively excluded
[g] Mixing ratio extracted assuming spin-parity 4^-
[h] No branching intensity could be determined; γ ray weaker member of unresolved doublet
[i] Transition not observed in the $(n, n'\gamma)$ reaction; branching ratio taken from Ref. [7]
[j] Transition observed in the $(n, n'\gamma)$ reaction, but branching ratio taken from Ref. [7]
[k] γ ray may be part of an unresolved doublet
[l] Placement uncertain

yielding $\tau = 180^{+190}_{-70}$ fs and the latter $\tau > 570$ fs. This may be due to feeding from higher-lying states, although in the present work the only transition with sufficient intensity to be observed feeding the 6_1^+ level is from the 5_1^+ state at 2927 keV that has a 8% γ-ray branch to the 6_1^+ level, and should not seriously perturb the measurement at $E_n = 3.2$ MeV. Thus, the cause of this inconsistency is unknown; the most likely explanation is the presence of an unresolved γ-ray doublet or background line, but there is no direct evidence for this. Nonetheless, it is deemed prudent to adopt the lifetime for the 6_1^+ level from Lobach et al. [45].

The evaluated lifetime [23] for the 1476-keV 2_2^+ level is 980±140 fs, based on the average of two Coulomb-excitation experiments [46,47] that deduced $B(E2\uparrow)$ of 0.021(3) e^2b^2 which converts to $B(E2; 2_2^+ \rightarrow 0_1^+) = 1.34(19)$ W.u. The lifetime published in Ref. [7] of $1.95^{+0.50}_{-0.33}$ ps is a factor of two longer resulting in $B(E2; 2_2^+ \rightarrow 0_1^+) = 0.68(14)$ W.u., closer to the results from the (e, e') reaction [48] which yielded $B(E2; 2_2^+ \rightarrow 0_1^+) = 0.9(2)$ W.u. A recent Coulomb-excitation study [38] yields a much more precise value of $B(E2; 2_2^+ \rightarrow 0_1^+) = 0.95(5)$ W.u. that results in a calculated lifetime of $\tau = 1.40^{+0.06}_{-0.08}$ ps. At the neutron energy used to determine the 2_2^+ level lifetime, $E_n = 2.6$ MeV, approximately 30% of the observed cross section is due to feeding from higher-lying states. Unfortunately, the greatest feeding contribution arises from the 0_4^+ level for which the lifetime cannot be extracted. However, the 0_4^+ lifetime must be rather long, > 10 ps, otherwise the $B(E2; 0_4^+ \rightarrow 2_3^+)$ value for the 295-keV transition would be unrealistically large. With this assumption, the $F(\tau)$ value for the 2_2^+ state can be recalculated and increases to 0.024(5) resulting in a lifetime of $1.6^{+0.7}_{-0.4}$ ps. Finally, the lifetime for the 2079-keV 3_1^- state is determined to be $\tau = 750^{+100}_{-80}$ fs, as obtained from the average of the $F(\tau)$ values extracted for the 1421-keV and 603-keV γ rays. The 1421-keV peak is due to a doublet of γ-ray transitions with the other member arising from the 2079-keV 0^+ state. The $F(\tau)$ value for the 603-keV transition, which has no observable branch from the 2079-keV 0^+ state [25], is 0.045(22) that is in excellent agreement with the 1421-keV $F(\tau)$ of 0.047(5) although the former has a very large uncertainty. The 1421-keV branch from the 2079-keV 0_4^+ state is weak and accounts for approximately 17% of the

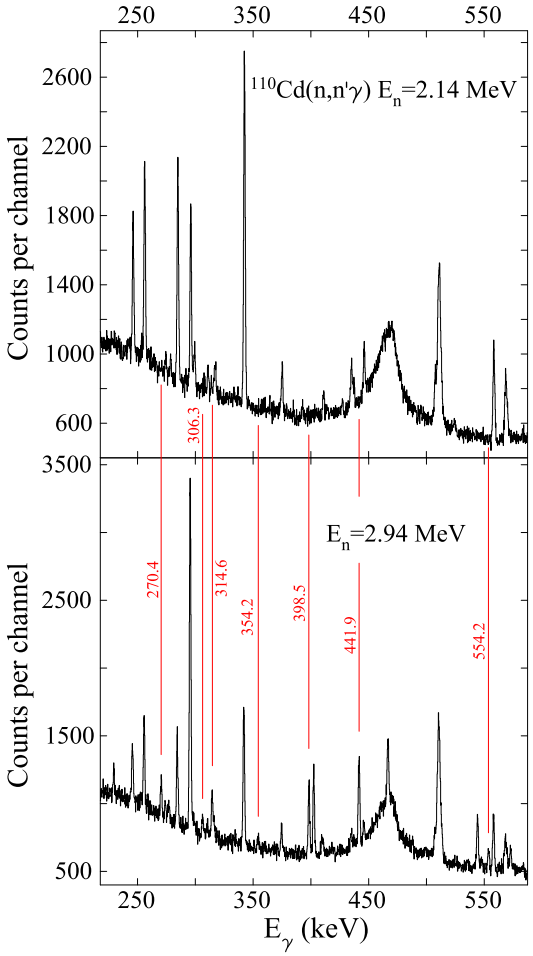

Fig. 2 Portions of the γ-ray spectra observed for neutron bombarding energies of 2.14 MeV (top) and 2.94 MeV (bottom). The red lines indicate newly-assigned γ-ray lines that were not reported in Refs. [10, 11] and are labelled with their energies in keV

total 1421-keV γ-ray intensity at 2.6 MeV. Using the same assumption as used above for the feeding of the 2_2^+ state, the $F(\tau)$ value can be corrected to 0.057(6) resulting in a lifetime of 630^{+90}_{-80} fs. While the assumption of the long lifetime of the 2079-keV 0_4^+ level is a reasonable one, we consider the corrected lifetime values as lower limits of our measurement.

The angular distributions of the γ rays emitted in the reaction are analysed using the results of calculated distributions from the Hauser-Feshbach code CINDY [49]. Figure 4 displays examples of the observed γ-ray angular distributions, fit with

$$I_\gamma(\theta_\gamma) = I_\gamma^0 \left(1 + a_2 P_2(\cos\theta_\gamma) + a_4 P_4(\cos\theta_\gamma)\right), \qquad (2)$$

as well as the resulting reduced χ_ν^2 distributions as a function of the multipole mixing ratio δ obtained from a comparison of the observed data to the CINDY calculations. Generally, the values of the mixing ratios and initial spins resulting in

Table 2 Additional γ rays, along with their threshold energies observed in the excitation functions, believed to belong to ^{110}Cd, which are not placed in the level scheme. All γ rays listed have intensities $I_\gamma < 0.2\%$ of the 657.8-keV $2_1^+ \rightarrow 0_{gs}^+$ transition. Their energies were measured with the HPGe detector at 125° with respect to the direction of the proton beam used to produce the neutrons and hence may have effects from Doppler shifts

E_γ (keV)	E_{th} (MeV)	E_γ (keV)	E_{th} (MeV)
253.0(1)	3.04	923.9(2)	3.34
356.24(5)	3.04	965.1(3)	3.34
360.0(2)	3.14	1024.1(2)	2.94
401.62(8)	3.24	1068.2(2)	3.34
495.2(2)	3.34	1220.8(2)	3.24
535.4(1)	3.24	1508.8(2)	3.04
650.90(6)	3.24	1601.4(2)	3.24
655.8(1)	3.34	1662.6(3)	3.34
667.3(2)	3.14	1666.0(1)	3.24
675.7(3)	3.34	1691.8(2)	3.24
849.1(2)	2.94	1739.6(2)	3.34
907.9(2)	3.04	1779.6(3)	3.34

χ_ν^2 values falling below the 99% confidence limit were considered. The spin assignments were made by combining the angular-distribution results for all known branches and the excitation functions, taking into account results from other experiments [23].

Shown in Fig. 5 are examples of excitation functions obtained. Those in the left panels are summed partial γ-ray cross sections for all γ rays assigned as decay transitions from the states indicated, whereas those in the right panels are the partial cross sections for individual γ rays. The excitation-function shapes and magnitudes are indicative of the spins of the states, with spin 1, 2, and 3 having the greatest magnitudes and similar very rapid rises in cross section once the energy threshold is exceeded. For higher-spin states, the cross sections increase more slowly as can be seen for the 937.5-keV and 628.6-keV cross sections. Information from the excitation functions is used for the placement of the γ-ray transitions in the level scheme, and augments that of the angular distributions for the determination of the level spins.

2.1 Discussion of individual levels

It has been well established that the $(n, n'\gamma)$ reaction, due to its statistical nature [50] for the neutron bombarding energies employed in this work, results in populations of levels that have little dependence on their particular structure. All levels with spin ≤ 6 are expected to be populated with sufficient cross section that they can be detected (see Fig. 14 of Ref. [15].) However, as the neutron bombarding energy increases, the resulting γ-ray spectra become increasingly

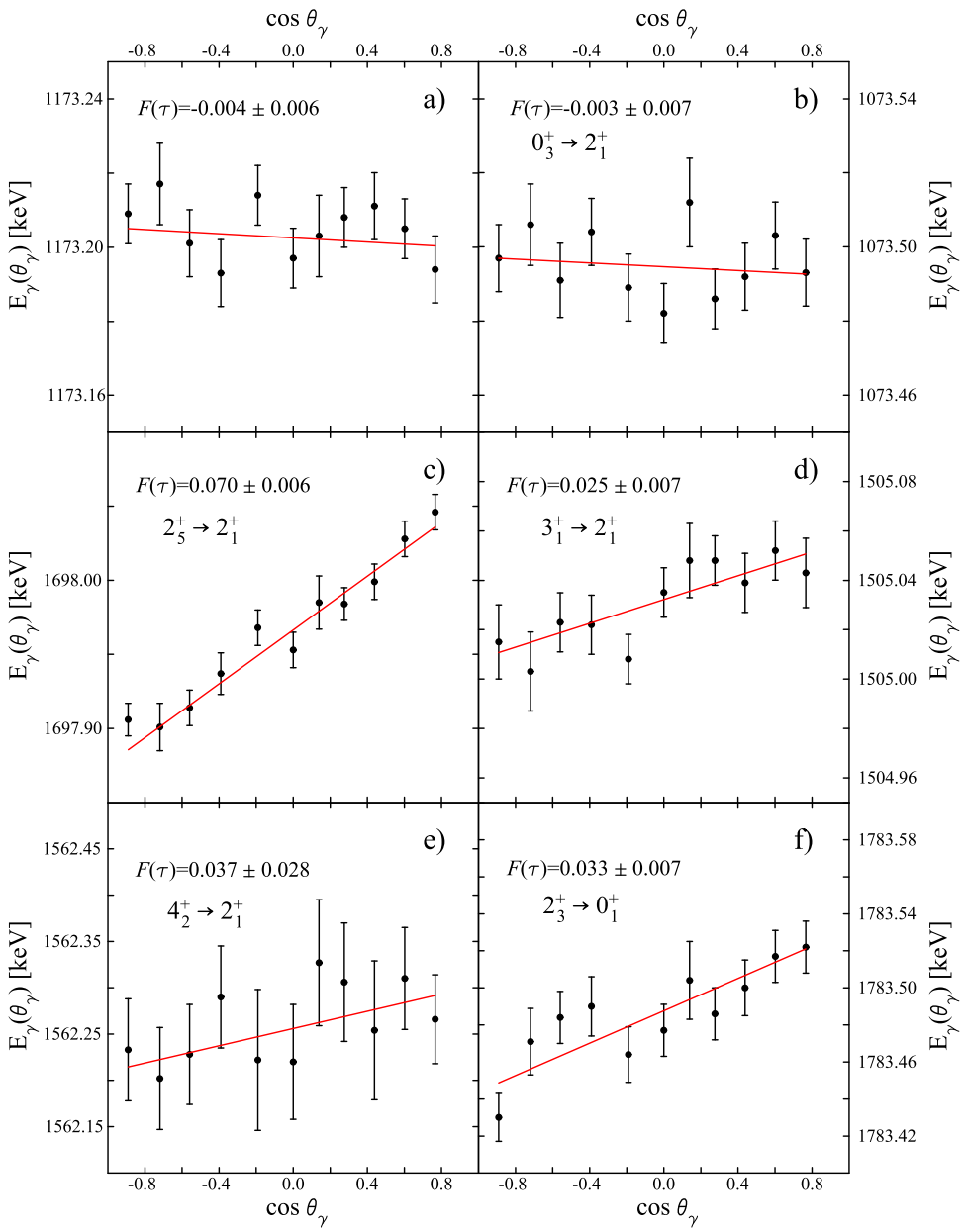

Fig. 3 Examples of Doppler shifts for selected transitions in the present analysis. The 1173-keV γ ray (panel a)) is from ^{60}Co, a source used to monitor the gain shifts of peaks in the spectra as the detector is positioned at different angles. The 1173-keV line was not used in the calibration; the $F(\tau) = -0.004 \pm 0.006$ is consistent with zero slope. The non-observation of a Doppler shift for the 1073.5-keV $0^+_3 \rightarrow 2^+_1$ transition (panel b)) gives a lower limit for the lifetime of 2 ps. Panels c) through f) show the observed Doppler shifts for the 1698.0-keV $2^+_5 \rightarrow 2^+_1$, 1505.0-keV $3^+_1 \rightarrow 2^+_1$, 1562.3-keV $4^+_2 \rightarrow 2^+_1$, and 1783.5-keV $2^+_3 \rightarrow 0^+_1$ transitions, respectively

complex; consequently, the detection of levels becomes more difficult and the probability of "missing" levels increases. This problem is exacerbated by the lack of $\gamma\gamma$ coincidence data obtained with the present $(n, n'\gamma)$ reaction. As outlined above, access to $\gamma\gamma$ coincidence data from the β decay of ^{110}In helps alleviate this problem somewhat, but the poor overlap in populated levels above $\approx$ 2.5 MeV results in a degraded confidence that all levels have been established above that energy. This is particularly true for those levels that do not decay to the ground state nor first excited 2^+ state. Nonetheless, some levels observed in other studies above 2.5 MeV in excitation energy can be confidently concluded not to exist. For these, we applied the criteria that their suggested spin was $I \leq 3$ or 4^+ in order to have a high likelihood to decay to either the ground state or the first excited 2^+ state, and thus easily observable. The levels concluded not to exist

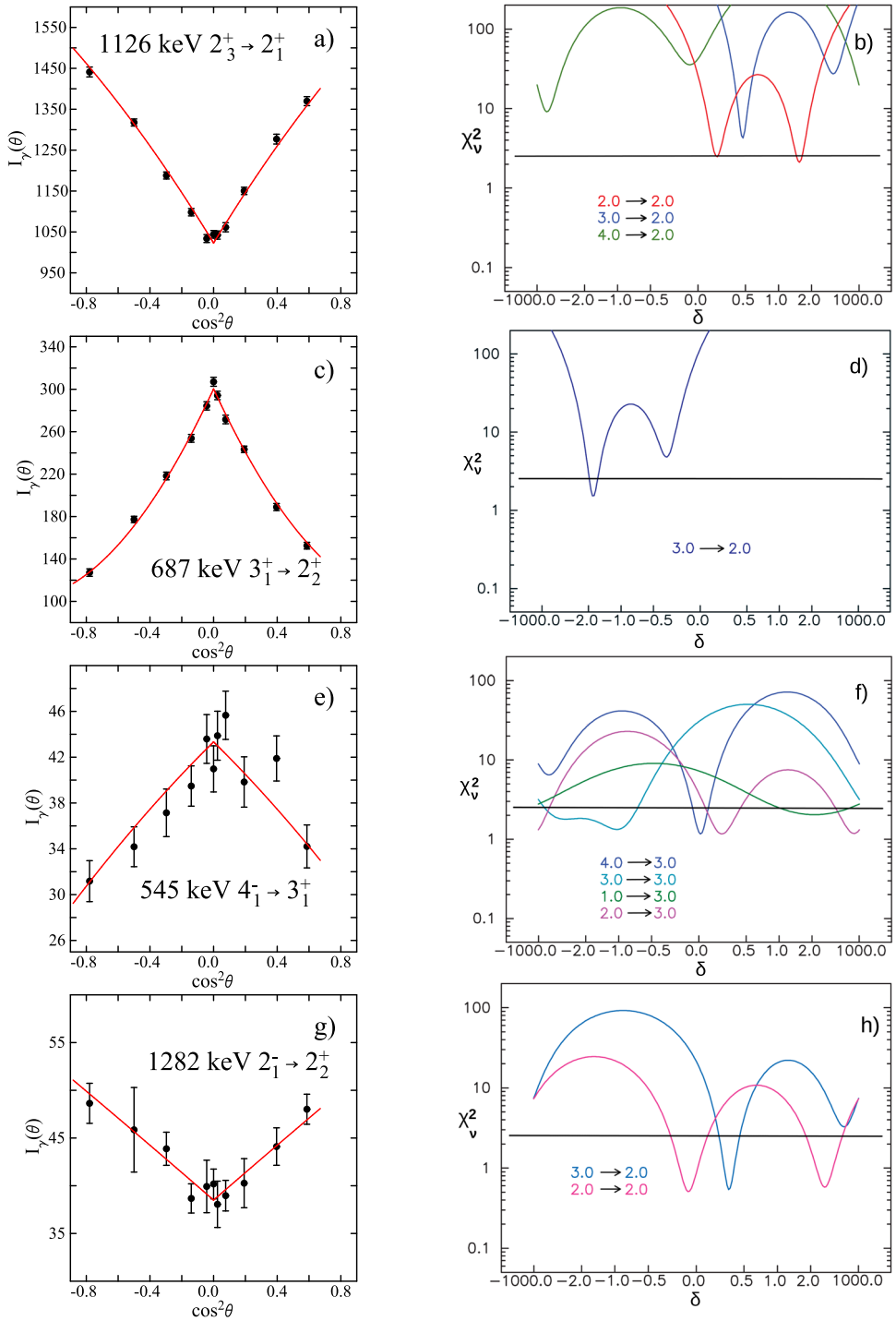

Fig. 4 Examples of angular distributions of γ rays observed in the present study. The left panels display the distributions plotted as a function of $\cos^2\theta$ where the negative sign indicates angles greater than 90°. The red curves are fits to the distributions described in the text. Transitions that are purely dipole have an absence of the $P_4(\cos\theta)$ term resulting in a linear dependence in these plots. The panels on the right display the χ^2_ν values resulting from comparisons with the results of CINDY calculations [49] of the angular-momentum alignments for the spins of the levels indicated as a function of the multipolarity mixing ratio δ. The horizontal lines indicate the 99% confidence level. In some cases, such as for the 687-keV $3_1^+ \rightarrow 2_2^+$ transition, the χ^2_ν values for other possible spin values are extremely large and exceed the plot scale

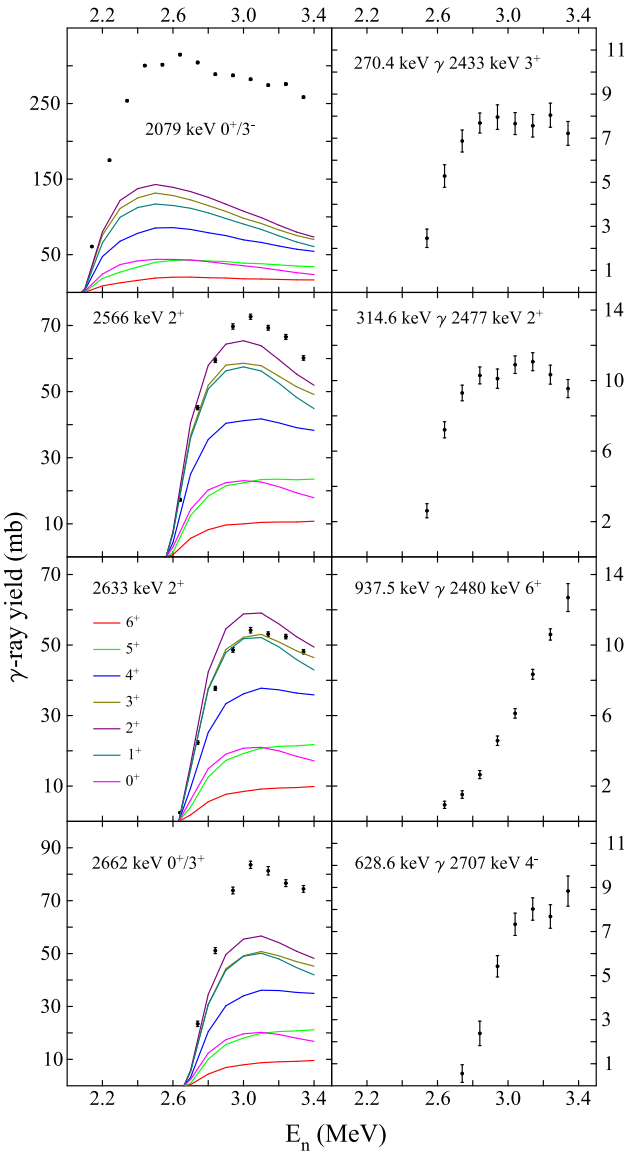

Fig. 5 Examples of excitation functions observed in the present study. The data have been normalized to the results of CINDY calculations such that the level cross sections for well characterised states agree with the calculated magnitude. The data in the left panels are the observed level cross sections compared with the predicted values for spins 0 – 6 (curves). The data displayed in the right panels are the individual γ-ray partial cross sections. The observation of a substantially greater cross section than predicted indicates the presence of a doublet of levels, as in the case of the 2079-keV $0_4^+/3_1^-$ doublet and the 2662-keV $0_6^+/3_4^+$ doublet, in contrast to the behavior of the 2356-keV and 2633-keV 2^+ level cross sections

are noted with a "n.o." in Table 1. Below, we discuss only a few of these non-observed levels to elaborate the process.

2.1.1 1809-keV 4^+ level

The existence of a level at 1809 keV was suggested in both an (e, e') reaction study [48] and in a ^{108}Pd$(\alpha, 2n\gamma)$ reaction study [24]. A β-decay study [51] performed shortly thereafter found no evidence of the 1809-keV level, and this level was not reported by Corminboeuf et al. [11] in their earlier $(n, n'\gamma)$ analysis. In agreement with those studies, no evidence is found in the present work for the existence of the 1809-keV level, and it is concluded not to exist.

2.1.2 2184-keV (1^-) level

In a (p, p') and (d, d') inelastic scattering study [52], a tentative 1^- state at 2184 keV was reported. No further evidence has been found for a 1^- state at this energy in any other study, including a (γ, γ') reaction [53]. No evidence for the existence of this level in the present work is found, and it is concluded not to exist.

2.1.3 2198-keV $2^+, 3^+$ level

A ^{111}Cd$(\mathbf{d}, t)^{110}$Cd study [54] (**d** stands for polarised deuterons) located a very weakly populated state at 2198 keV, with a spectroscopic factor for $d_{5/2}$ transfer of $S = 0.002$. No evidence is found for this level in the present study, and it is concluded not to exist.

2.1.4 Levels near 2.4 MeV

A series of levels were observed as very weak peaks in the ^{111}Cd$(\mathbf{d}, t)^{110}$Cd reaction (2365 keV and 2381 keV) [54] and the inelastic scattering (p, p') and (d, d') reactions (2377 keV, 2385 keV, 2405 keV) [52]. No other experiment has observed these levels, a result consistent with the present work. No evidence of possible decay γ rays was obtained in the excitation functions or the angular distributions. It is concluded that these previously assigned levels resulted from target impurities in the transfer and scattering reactions, and that the levels do not exist.

2.1.5 2433-keV 3_2^+ level

Both the inelastic scattering and $(\mathbf{d}, t)$ experiments [52,54] report a level at 2432 keV; the presence of $d_{3/2}$ in the single-neutron transfer population, together with the much stronger $d_{5/2}$ component, indicates 2^+. A 3^+ level at 2433 keV is listed in the Nuclear Data Sheets [23] and is observed in the present study. It is suggested that this corresponds to the peak observed in the $(\mathbf{d}, t)$ reaction, and that the $d_{3/2}$ component in the transfer is spurious. (It should be noted that in the case of a pure $l = 2$ transfer, the decomposition of the $d_{3/2}$ and $d_{5/2}$ components is a result of a fit to the analysing powers only.) The present study also finds no evidence for a possible 651-keV γ-ray decay from the 2433-keV level to the 1783-keV 2^+ state. The excitation function for the 651-keV γ ray, rather, indicates a threshold above 3.1 MeV. Newly observed

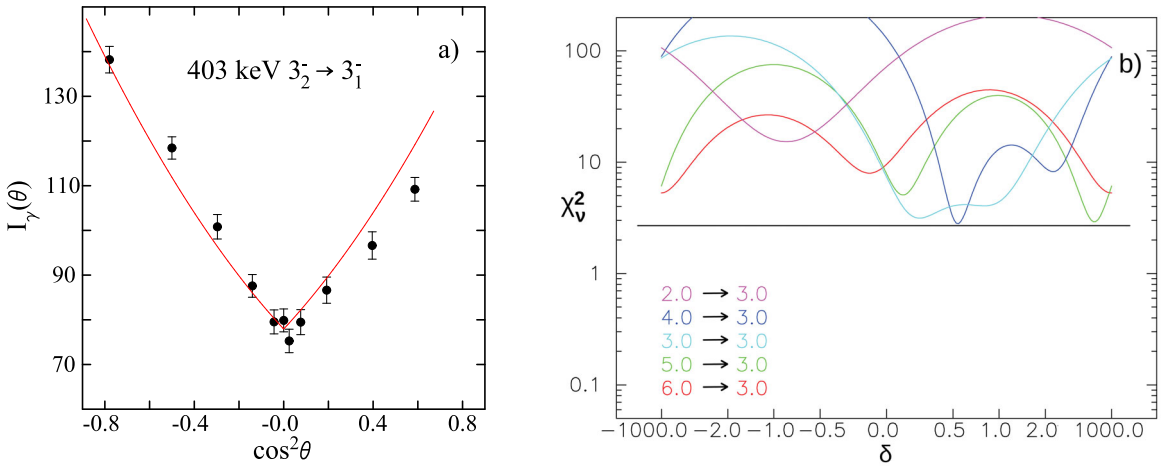

Fig. 6 Angular distribution plotted as a function of $\cos^2\theta$ (panel a)) of the 403-keV γ ray assigned as the transition from the 2481-keV state to the 2079-keV 3^-_1 state. The red curve is a fit to the distributions described in the text. Panel b) displays the χ^2_ν values resulting from comparisons with the results of CINDY calculations [49] of the angular-momentum alignments for the spins of the levels indicated as a function of the multipolarity mixing ratio δ. The horizontal line indicates the 99% confidence level. While all of the χ^2_ν curves are above the 99% confidence level, that for spin 2 is exceedingly large and this spin assignment is definitely excluded

decaying transitions of 270.4 keV (see Fig. 5) and 354.3 keV are unambiguously placed.

2.1.6 2481-keV 3^-_2 level

A level at 2481 keV was previously suggested to be 3^- in the (p, p') and (d, d') inelastic scattering measurements [55], but a 2^+ assignment was favoured in the study by Corminboeuf et al. [11] largely due to the excitation function having a better agreement with the calculations for spin 2 *vs.* spin 3. In the present work, the excitation functions are not judged as able to differentiate between the spin 2 or 3 solutions. The angular distributions of the 698-, 1006-, and 1824-keV γ rays permit both spin-2 or spin-3 solutions, where for spin 2 they would imply a mixed $E2+M1$ character, and for spin 3 result in a mixing ratio consistent with 0. The 403-keV transition, on the other hand, has no acceptable solution for spin 2, and for spin 3 results in a minimum in the χ^2 distribution for a mixed multipolarity as shown in Fig. 6. We thus adopt the spin assignment of Pignanelli et al. [55] of 3^-. As shown in Fig. 8, the 3^- assignment for the 2481-keV level fits extremely well with the systematics of the 3^-_2 states in the Cd isotopes.

2.1.7 2566-keV 3^+_3 level

A level at 2566 keV was assigned as having either 2^- or spin 3 with two γ-ray decays placed; a 783-keV γ-ray to the 1783-keV 2^+ level, and a 1909-keV γ ray to the 658-keV 2^+ level. In the present work, we re-assign the 1091-keV γ ray previously placed as a decay transition from the 2633-keV 2^+_7 level, as a decay transition from the 2566-keV 3^+_3 level. While the γ-ray energy (1090.654(7) keV) strongly favours its placement as the 2566.468(18) keV → 1475.806(11) keV transition, strong evidence also comes from the examination of the observed Doppler shifts. Figure 7 displays the Doppler shifts of the transition energies for the strongest decay branches from the 2633-keV level – the 1975-keV γ ray – and from the 2566-keV level – the 1909-keV γ ray. A clear difference in their $F(\tau)$ values is observed indicating that they originate from different levels. The observed Doppler shift of the 1091-keV γ ray perfectly matches that of the 1909-keV γ ray and is clearly not in agreement with that of the 1975-keV γ ray. While we cannot set an upper limit on the existence of a possible 2633-keV→1542-keV γ-ray transition with the present data, we also have no evidence for its existence.

2.1.8 2662-keV $0^+_6/3^+_4$ levels

In a ^{110}Ag β-decay study, Kawase et al. [57] assigned 0^+ to a level at 2662 keV based on an angular-correlation analysis that clearly indicated a $0^+ - 2^+ - 0^+$ cascade for the 2004 keV/658 keV pair of γ-ray transitions. Later, the single-neutron-transfer work by Blasi et al. [54] populated a level at 2662 keV with $d_{5/2}$ ($S_{d_{5/2}} = 0.052$) and $g_{7/2}$ ($S_{g_{7/2}} = 0.631$), indicating a 3^+ assignment. The previous $(n, n'\gamma)$ analysis [11] found that the angular distributions of the γ-rays de-exciting the 2662-keV level were consistent with a 3^+ assignment, an observation shared in the present work. However, the γ-ray yields greatly exceed that expected for a single 3^+ level (see Fig. 5) and clearly indicates that a doublet of levels

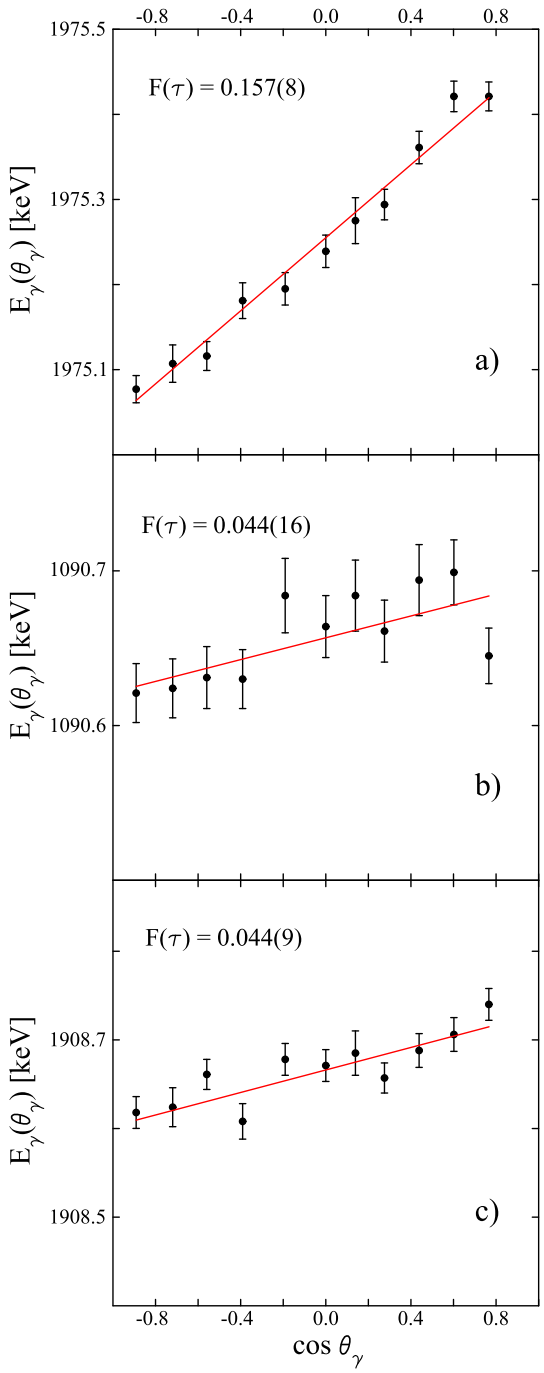

Fig. 7 Doppler shifts for the 1975-keV γ ray from the 2633-keV 2^+_7 level (top) and the 1909-keV γ ray from the 2566-keV 3^+_3 level (bottom). The middle panel displays the Doppler shift observed for the 1091-keV γ ray. The vertical scales have been adjusted to span a constant $\Delta E/E$ range so that the slopes as a function of $\cos\theta$ can be directly compared. The Doppler shift of the 1091-keV γ ray matches that of the 1909-keV γ ray, supporting its placement as a decay transition from the 2566-keV 3^+_3 level

is present at 2662 keV, for which spin-parities 0^+ and 3^+ are adopted. As decays of both 0^+ and 3^+ levels may populate lower-lying 2^+ levels, these transitions are highly likely to be doublets that cannot be resolved in the present work. In fact, both the 1186-keV and 2004-keV γ-ray peaks show evidence for doublet natures with peak centroids that shift with neutron energy. As a result, the data listed in Table 1 do not report branching ratios, nor mixing ratios for transitions feeding the 2^+ states, as these depend on the specific population ratio of the 3^+ and 0^+ levels.

2.1.9 2706-keV 4^+_5 and 2707-keV 4^-_1 levels

Two levels that occur very close in energy exist at 2705.7 and 2707.4 keV. In the $(\alpha, 2n\gamma)$ study by Kern et al. [24], both levels were observed and assigned as spin 4, with the lower level suggested to be negative parity and the 2707-keV level assigned positive parity. The negative-parity suggestion [24] for the 2706-keV level is based primarily on the observation of a mixing ratio for the 1163.2-keV transition of $\delta = 0.0(3)$ [24]. The 2707-keV level, on the other hand, was assigned 4^+ due to its observed mixed $M1+E2$ 545-keV transition to the 3^+ level at 2163 keV, with a value of the mixing ratio of $\delta = 0.21(11)$ [23]. The previous $(n, n'\gamma)$ analysis resulted in an assignment of both levels as 4^+ [11], as did the decay study of the 6^+ ^{110}Ag isomer ($t_{1/2} = 250$ d) [23], reporting on the existence of a 1.6-keV $M1$ transition [56]. In the present work, the 1163.2-keV γ ray to the 4^+_1 state has two possible values for the mixing ratio; $-1.18^{+0.20}_{-0.18}$ and $-0.04(7)$, with the former value favoured, thus implying a 4^+ assignment. A 4^+ assignment is also in agreement with results of a β^+/EC-decay experiment [6,7] that established a weak decay branch feeding the 2287-keV 2^+ level, and that the 2705.7-keV state is fed by a transition from the 3340-keV 6^+ state, leading to the 4^+ assignment. This branch will be important for the interpretation of these states outlined below.

The previous 2707-keV level 4^+ assignment is based on two facts; 1) the 545-keV transition, from Ref. [24], is of mixed character, and 2) the 1.6-keV transition to the 2705.7-keV level is of $M1$ character. In the present work, the 545-keV γ ray is observed and placed depopulating the 2707.4-keV level. However, its angular distribution, shown in Fig. 4, is consistent with a pure dipole transition. The 628.6-keV γ ray, on the other hand, appears to be of mixed character, which would imply a negative parity for the 2707.4-keV

level. Postulating that the 2705.7-keV and 2707.4-keV levels have opposite parity would also remove the highly curious result of two levels with the same spin and parity being only 1.6 keV apart, limiting any possible mixing matrix element to be less than 0.8 keV.

Further support for the negative-parity assignment of the 2707.4-keV level is based on the systematics of known negative-parity states in the even-even Cd isotopes. Shown in Fig. 8 are the energy systematics observed for the lowest-energy negative-parity states. Smooth trends, especially for the 2^-, 3^-, and 4^- states are observed; if any other potential candidate for the 4^-_1 level were adopted, it would result in a strong kink in an otherwise smooth curve. The inelastic scattering study by Pignanelli et al. [55] also assign $I^\pi = 4^-$ to the level at 2708 keV. The assignment of opposite parities to the 2705- and 2707-keV levels, however, it is at odds with the $M1$ character for the 1.6-keV transition assigned [23] as depopulating the 2707-keV level. A re-investigation of this transition is thus called for.

2.1.10 2758-keV 2^-_1 level

A previously observed level at 2758.2 keV was assigned as $(1, 2, 3)^+$ based on the observation of a mixed $E1/M1$ character for the 1282.5-keV γ ray in an earlier $(n, n'\gamma)$ reaction [58]. The 1282.5-keV γ ray was also observed in the $(\alpha, 2n)$ reaction [24], but possessed an angular distribution consistent with that of a pure dipole. In the present study, the 1282.5-keV γ ray is consistent with a pure dipole, as shown in Fig. 4. The (p, p') and (d, d') reactions reported by Pignanelli et al. [55] indicated the presence of a 2^- state at 2757 ± 3 keV. This spin-parity assignment is consistent with the present data, and thus $I^\pi = 2^-$ is adopted. As seen in Fig. 8, this assignment fits well with the energy systematics of known 2^- states in the even-even Cd isotopes.

2.1.11 2916-keV and 2917-keV levels

A level at 2917.6 keV with possible spin and parity assignment of 2^+, $3^\pm$, 4^+ was previously established, observed in the $(n, n'\gamma)$ reaction [11] with spin 2^+, 3^- favoured, and in inelastic scattering [52] where a 4^+ assignment was made for a level at 2915 ± 3 keV. In the most recent evaluation for ^{110}Cd [23], the 2917.6-keV level was assigned three decaying transitions; 356.4 keV, 1441.9 keV, and 2259.5 keV. In the present study, a doublet of levels are assigned at 2916.3 keV and 2917.6 keV. The lower member of the doublet has five decaying transitions assigned; 837.5 keV, 1132.8 keV, 1373.8 keV, 1440.5 keV, and 2258.6 keV, and is favoured to have spin-parity 3^+. The upper member of the doublet has decay γ rays of 667.3 keV and 1375.5 keV, and a 4^+ assignment is favoured from the both the shape and magnitude of the excitation functions. No evidence is found for the placement of a 356-keV γ ray from either of these levels, and the 1441.9-keV transition we observe is placed from the 2984.6-keV level. This latter assignment is based on its excitation function, and is confirmed in the β-decay study [44].

2.1.12 3043-keV levels

The $(\mathbf{d}, t)$ study of ^{110}Cd [54] located both $s_{1/2}$ and $l = 2$ strength[2] at 3040(3) keV. Based on the observed strength, a doublet of levels was suggested with I^π values of 0^+ and 2^+ or 3^+. A (γ, γ') study [53] determined the existence of a 1^+ level at 3043 keV. In the present study, a doublet of levels is also suggested with γ-ray transitions of 3043.4 keV, 2385.9 keV, 1569.9 keV and 1566.9 keV. The 3043.4- and 1569.9-keV γ rays are assigned exclusively to the 1^+ state, and the energy of the 1^+ state listed in Table 1 is derived from them. The 2385.9-keV and 1566.9-keV γ rays can originate from either state; we list them as originating from the 0^+ state but it should also be noted that the 2385.9 keV energy matches better to the 1^+ state than when paired with the 1566.9-keV γ ray. An examination of the branching ratios of the 2385.9- and 1566.9-keV transitions as a function of the neutron bombarding energy suggests that there may be branches of these transitions as well from the 1^+ state. However, the lack of $\gamma\gamma$ coincidences in the present study prevents the confirmation of this suggestion.

3 Discussion and interpretations

At low excitation energies, it is anticipated that the states are collective in nature, either based on surface vibrations or rotations, or pairing degrees of freedom. Traditionally, the mid-shell Cd isotopes have been interpreted as having a spherical shape and possessing vibrations (see, e.g. Ref. [3,59]), but recent work [6,7] suggested that ^{110}Cd exhibits multiple shape coexistence and that the states are rotational in nature.

The study conducted in Ref. [25] focused on the previously assigned [10,11,24] one-, two-, and three-phonon states. Briefly, it was found that calculations within the strong-mixing scenario [28,29], while able to reproduce the decays at the two-phonon level, also predicted enhanced transitions between states dominated by the intruder configuration and states predominately of the spherical multi-phonon config-

[2] In Table 2 of Ref. [54], there are a number of incorrect listings for higher-excitation energy states. For example, for the 3040-keV doublet peak, possible spins of 2^+, 3^+ are listed, while the strength is given in the $d_{3/2}$ column. Since the target has spin $\frac{1}{2}^+$, if the strength was for the $d_{3/2}$ configuration, only spins of 1^+, $2^\mp$ would be allowed. In such situations, which occurs almost exclusively for weakly populated states, it is considered that there is evidence for $l = 2$ strength, but that the analysing powers are not sufficiently conclusive to determine the j value of the transfer.

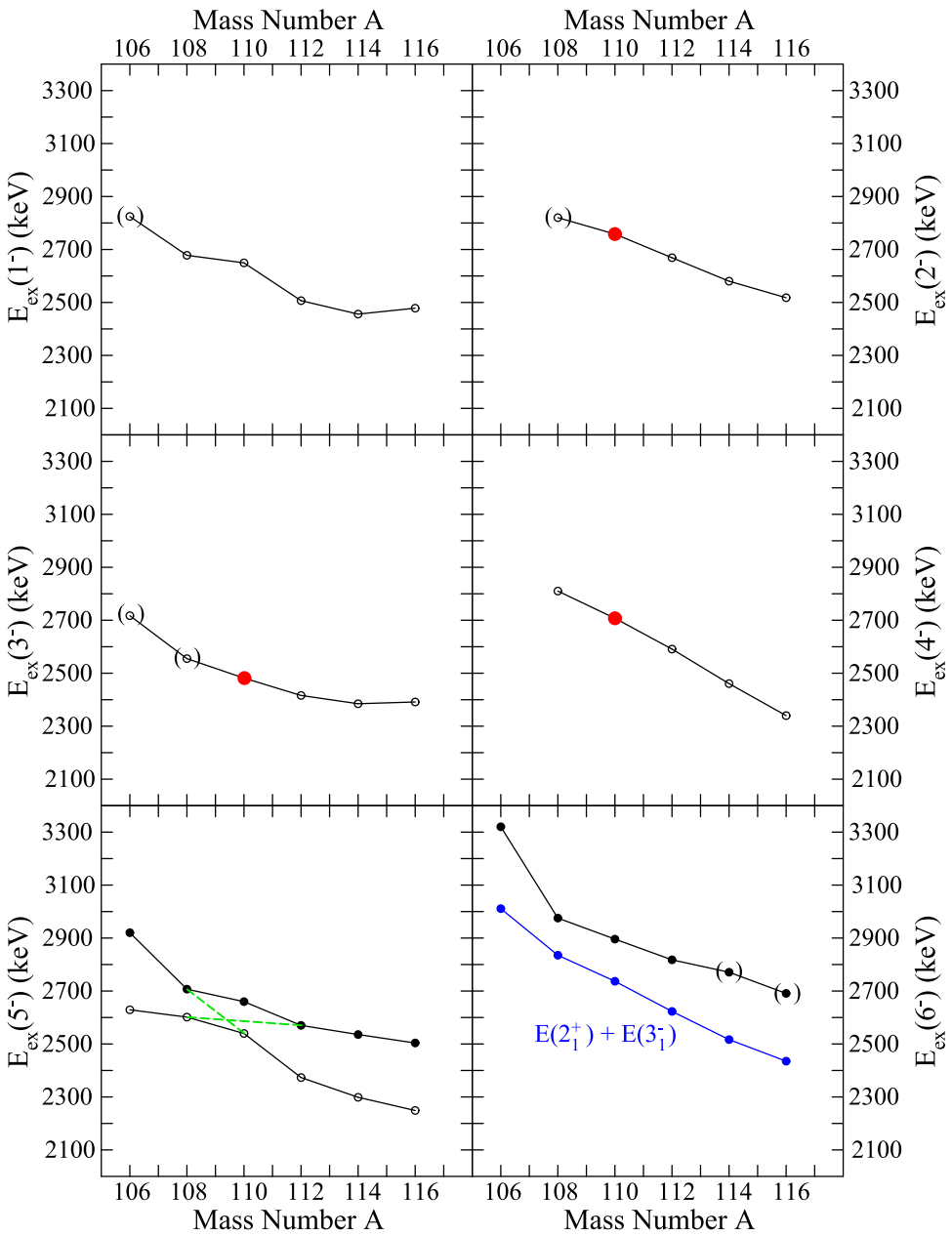

Fig. 8 Energy systematics of the low-lying negative-parity states in ^{106}Cd–^{116}Cd. Points surrounded by parentheses do not have firm spin or parity assignments. The blue curve displayed on the plot for the 6^-_1 level energy systematics is the sum of the energies of the 2^+_1 and 3^-_1 states. The points in red for ^{110}Cd indicate either a new spin and parity assignment, or a further clarification of the level and/or spin. The energies of the second 3^- state, and both the 5^-_1 and 5^-_2 levels, are plotted. The green dashed lines connecting the 5^- states are connecting levels suggested to have the same character, with a crossing of the nature of the levels occurring at ^{110}Cd

uration. These cross-configuration transitions were found experimentally, however, to be either very weak or non-existent, except those from the intruder-band head to the 2^+_1 level, and the 6^+ member of the ground-state band to the 4^+ intruder-band member. This observation refuted the strong mixing between the configurations, thus removing the explanation of the decays of the 0^+_2 and 0^+_3 states, requiring an alternative explanation to be sought. Systematically, in the Cd isotopes near the neutron mid-shell, the first excited 0^+ non-intruder state (0^+_3 in ^{110,112,114}Cd and 0^+_2 in ^{116}Cd) has a strongly enhanced $B(E2)$ value for decay into the 2^+_2 state, and an extremely weak decay to the 2^+_1 level, a pattern suggestive of γ-soft behavior. Further, as Fig. 10 displays for ^{110}Cd, the "quasi-γ band" has a staggering consistent with that of a γ-soft rotor.

In order to deduce which levels may possess a collective character, ideally the presence of enhanced $B(E2)$ values is used. However, in many cases the in-band $E2$ transitions compete with high-energy interband transitions such that they have extremely small branching ratios falling below the observational limit. This situation creates uncertainty in the assignment of states. We first consider those states that can be identified as being predominately two-quasiparticle in nature.

3.1 Two-quasiparticle configurations

There have been two single-nucleon-transfer experiments performed populating levels in ^{110}Cd [54,60], limited by the available stable targets. States that are strongly populated in the reactions must predominantly have a two-quasiparticle configuration for their wave functions since the ground states of the odd-A targets are dominated by a one-quasiparticle configuration. Further information on two-quasiparticle states can be ascertained from the strong transitions observed in β decay feeding levels in ^{110}Cd. A strongly populated state would not have a wave function dominated by multiphonon components; however, a one-phonon state can still be dominated by a single two-quasiparticle configuration leading to a strong transfer population.

If the target and final nuclei have spherical shapes, the single-particle states have a $(2j+1)$-fold degeneracy and we would only observe a limited number of states populated with large transfer strengths. For deformed systems, a Nilsson model type approach is far more appropriate with the single-particle states splitting into $(2j+1)/2$ levels with transfer strengths of $S \approx 1$ times the square of the appropriate Clebsch-Gordan coefficient. In the discussion below, we use this expectation to make assignments of levels with a predominantly two-quasiparticle configuration.

3.1.1 Proton two-quasiparticle configurations

The single-proton-transfer study by Auble et al. [60] located the proton two-quasiparticle states coupled to the $(p_{1/2})^{-1}$ single-particle configuration of the ^{109}Ag target. It was found that the strongest peaks were located in the vicinity of 3.7 MeV, and were predominately populated with $l=2$ transfer, presumably associated with the $d_{5/2}$ orbital. The strongest $l=2$ transfer is to a level at 3812 keV with a spectroscopic strength of 1.1 [60]. Of the levels below 3 MeV, the ground state was the strongest populated with an $l=1$ transfer that largely exhausts the available $p_{1/2}$ strength with a spectroscopic factor of 0.75 [60]. The first excited 2^+ state is also significantly populated, indicating a substantial emptiness of the $p_{3/2}$ orbital (the measured spectroscopic factor is $S=0.21$ [60]) even at $Z=48$. The 5^- state at 2539 keV is rather strongly populated with $S=0.41$ for $l=4$ [60], indicating a sizable component of the $(p_{1/2})^{-1}\otimes(g_{9/2})^{-1}$ configuration in its wave function. However, an even stronger $l=4$ strength, with a small amount of $l=0$ strength, was reported for a state at 2652 keV, originally believed to be due to a $(0^-, 1^-)$ and $(4^-, 5^-)$ doublet [60]. The improved knowledge of the level scheme now reveals that this strength is indeed due to two levels; the 1^-_1 state at 2650 keV and the 5^-_2 level at 2660 keV.

Levels in ^{110}Cd can also be populated via the β decay of the ground states and isomeric states of both ^{110}Ag and ^{110}In. Due to the one-body nature of the β-decay operator, if the parent configuration is known and there are allowed unhindered transitions (generally, having $\log ft \leq 5$), the daughter state wave function must involve a large degree of overlap. The decay of the ^{110}Ag ground state, with $I^\pi = 1^+$ and a configuration $\frac{7}{2}[413]_\pi \otimes \frac{5}{2}[413]_\nu$, has allowed-unhindered transitions to the ^{110}Cd ground state ($\log ft = 4.66$) and the 0^+_6 state at 2662 keV ($\log ft = 4.83$) [23]. All other 0^+ states have much larger $\log ft$ values. The decays to the 0^+ states must involve a spin-flip Gamow-Teller transition, and thus are sampling the $\pi(g_{9/2})^{-2}$ configuration; it can thus be stated with confidence that the 0^+ $\pi(g_{9/2})^{-2}$ configuration is predominately shared amongst the ground state and the 2662-keV excited 0^+ state. The strongest transition observed in the decay of the ^{110}Ag 6^+ state, with a configuration of $\pi g_{9/2}\otimes \nu g_{7/2}$ is to the 5^+ level at 2926 keV with a $\log ft = 5.365(25)$ indicating a component of the $g_{9/2}\otimes g_{7/2}$ two-proton configuration, but this is unlikely to be the dominant component of the wave function.

Combining the results of the β decay and the single-proton transfer, it is seen that the proton part of the ground-state wave function is dominated by the configuration $(p_{1/2})^{-2} + (g_{9/2})^{-2}$. The situation just below the $Z=50$ shell closure is very similar to that at the $Z=40$ subshell closure, where the ground state of is a nearly equal admixture of the $(p_{1/2})^2 + (g_{9/2})^2$ configurations, assuming ^{88}Sr as a core [61,62].

3.1.2 Neutron two-quasiparticle configurations

The $(\mathbf{d}, t)$ transfer study performed by Blasi et al. [54] achieved a high resolution and high sensitivity. Using a ^{111}Cd target, with the odd neutron in the $s_{1/2}$ state, the expected two-quasiparticle states populated are 0^+ $(s_{1/2}\otimes s_{1/2})$, $1^+, 2^+$ $(s_{1/2}\otimes d_{3/2})$, $2^+, 3^+$ $(s_{1/2}\otimes d_{5/2})$, $3^+, 4^+$ $(s_{1/2}\otimes g_{7/2})$, and $5^-, 6^-$ $(s_{1/2}\otimes h_{11/2})$. The (d,t) reaction [54] populates many more states indicating a large degree of fragmentation of the strength, especially the $d_{3/2}$ and $d_{5/2}$ configurations. There are particularly strong populations of the ground state ($S_{s_{1/2}} = 0.93$), and levels at 2563 and 2662 keV with $S_{g_{7/2}} = 0.59$ and 0.63, respectively [54]. The neutron part of the ground-state wave function is clearly dominated by the $(s_{1/2})^2$ configuration. The strong peak at 2563 keV in the (d,t) spectrum [54] could be due to both the 4^+_4 state at 2561 keV and the 3^+_3 state at 2566 keV. Since the 3^+_4 state at 2662 keV is strongly populated, the 4^+_4 state at 2561 keV is favoured to be responsible for the strength observed. Thus, the 3^+ and 4^+ states of the $s_{1/2}\otimes g_{7/2}$ configuration are assigned at 2663 keV and 2561 keV, respectively. The largest value observed for the $d_{5/2}$ strength was assigned to a 2^+ state at 2433 keV with $S_{d_{5/2}} = 0.23$ [54]. However, as outlined above, it is suggested that this level is the 3^+_2 state, and the extracted $d_{3/2}$ strength of 0.073 [54] should

be combined with the $d_{5/2}$ strength of 0.230 yielding a total strength of ≈ 0.3. The 3^+ member of the $\nu s_{1/2} \otimes d_{5/2}$ configuration is assigned at 2433 keV. The 2^+ member cannot be assigned since no state receives a significant fraction of the $d_{5/2}$ strength.

The decay of the 7^+ ^{110}In parent feeds strongly three states in ^{110}Cd; the 6^+ state at 3122 keV with $\log ft = 4.717(20)$, the 8^+ level at 3187 keV with $\log ft = 4.806(25)$, and the 6^+ level at 3525 keV with $\log ft = 5.04(4)$ [23]. With a dominant configuration for the 7^+ parent of $\pi(g_{9/2})^{-1} \otimes \nu d_{5/2}$, the final states with allowed-unhindered transitions populated can have the $g_{7/2} \otimes d_{5/2}$ two-neutron configuration. This would explain one of the strongly populated 6^+ states. It has been suggested [63], however, that the 7^+ ^{110}In parent also involves the $\pi(g_{9/2})^{-1} \otimes \nu g_{7/2}$ configuration, and thus could have allowed-unhindered transitions to the $\pi(g_{9/2})^{-2}$ configuration in the daughter states. The 3187-keV 8^+ level was assigned as the $K^\pi = 8^+$ $\pi(g_{9/2})^{-2}$ configuration [63], but a 6^+ state with the $\pi(g_{9/2})^{-2}$ should also be populated. Of the two 6^+ states observed to be strongly populated, the lower-energy 6^+ state at 3122 keV is favoured to have the $\pi(g_{9/2})^{-2}$ configuration.

In ^{112}Cd, a study [64] with the ^{111}Cd($\mathbf{d}$, p) reaction located the $\nu s_{1/2} \otimes h_{11/2}$ configuration with the 5^- member at 2373 keV, and the 6^- state at 2818 keV. This configuration was weakly populated in the ^{113}Cd(d, t) reaction, but had the largest spectroscopic strengths observed in the (d, p) reaction. It is suggested, based on the energy systematics presented in Fig. 8, that the 5^-_1 level at 2540 keV and the 6^-_1 level at 2895 keV have a dominant $\nu s_{1/2} \otimes h_{11/2}$ configuration in ^{110}Cd. It is also noted that the 2540 keV state was populated in the ^{109}Ag(^{3}He, d) reaction with an $l = 4$ spectroscopic strength of 0.4, implying a sizable component of the $\pi p_{1/2} \otimes g_{9/2}$ configuration.

Shown in Fig. 9 are the levels assigned as having substantial two-quasiparticle configurations in their wave functions, as deduced from the transfer reactions and β-decay experiments.

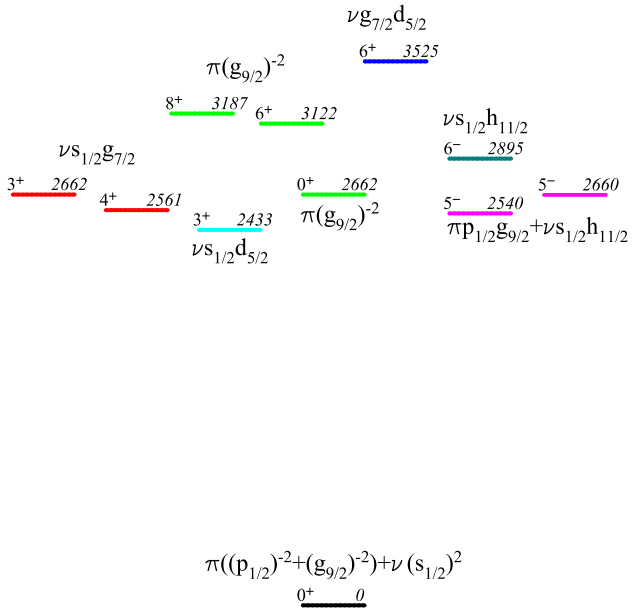

Fig. 9 Levels in ^{110}Cd that are assigned as possessing significant two-quasiparticle character. See text for details

3.2 The $K^\pi = 0^+_3$ band

In Refs. [6,7], the 0^+_3 state at 1731 keV was suggested to be the head of an oblate band, with the 2^+ band member at 2356 keV that has an enhanced $B(E2; 2^+ \rightarrow 0^+) = 24.2(22)$ W.u. [25]. Since the $2^+ - 0^+$ spacing is 624 keV, very similar to that of the ground-state band, we can take the $4^+ - 2^+$ ground-state band energy difference for guidance for the location of the 4^+ band candidates, suggesting that the 4^+ band member should be at approximately 3.2 MeV excitation energy. Unfortunately, at this excitation energy the present data do not have sufficient sensitivity for characterisation of 4^+ states.

3.3 The 0^+_4 state

In Ref. [6,7], the 0^+_4 state at 2079 keV was suggested to be the head of a deformed band. This was based on the observation of the systematic strong preference in $^{110-116}$Cd of the 0^+_4 state to decay to the 2^+ member of the 0^+_2 (^{110,112,114}Cd) or 0^+_3 (^{116}Cd) intruder band. The energy systematics of the 0^+_4 level displayed a characteristic "V-shaped" pattern, following those of the lower intruder states. If it is indeed the case that the 0^+_4 level is the band head, it can be expected that there should be accompanying rotational band members. There are several candidates for the 2^+ member; the 2287.5-keV, 2477.4-keV, 2633.2-keV, and 2787.5-keV states. These would yield rotational spacings of 209, 399, 544, and 708 keV, respectively. The 398.5-keV and 544.2-keV γ rays are assigned as decay transitions from the 2477.4-keV and 2633.2-keV states, respectively. From the analysis of β-decay data [44], these γ rays are placed as feeding the 2079-keV 3^-_1 level rather than the 0^+_4 level. Thus, no assignment of the rotational band based on the 0^+_4 state can be made at present.

3.4 $K^\pi = 2^+$ bands

Shown in Fig. 10 are the low-lying positive-parity levels in ^{110}Cd with the enhanced or dominant $E2$ transitions. The level sequence of 2^+_2, 3^+_1, 4^+_3, 5^+_1, and 6^+_3 has been assigned [6,7,24] as a $K^\pi = 2^+$ "γ" band built on the ground state. The 2^+, 3^+, and 5^+ members are in agreement with the assignment of Sakai [65]. The 4^+ member was suggested

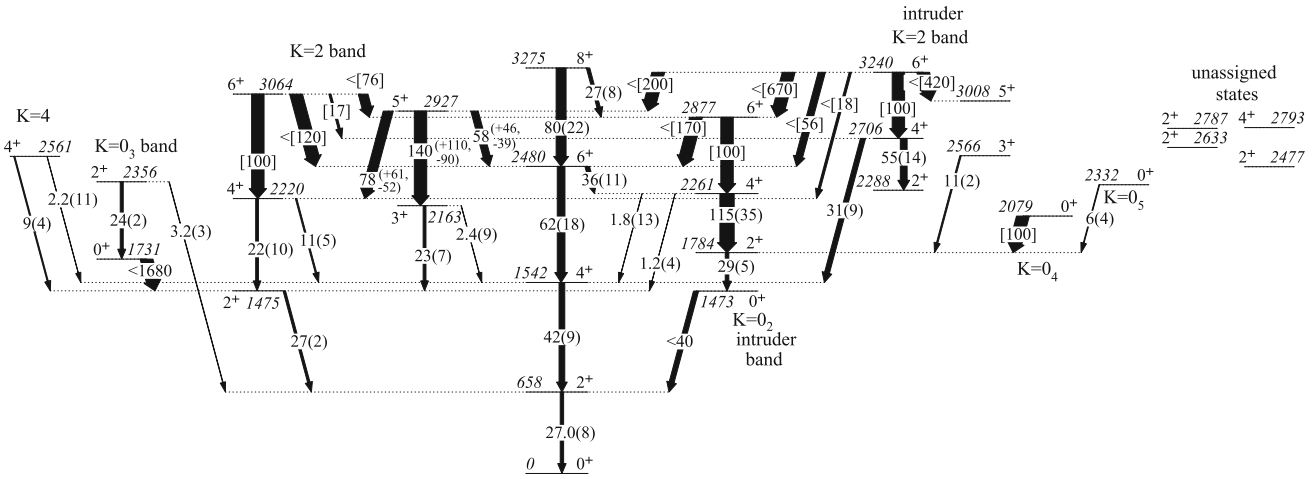

Fig. 10 Partial level scheme for ^{110}Cd for positive-parity states arranged into bands. Transitions are labeled with their $B(E2)$ values in W.u. with uncertainties in parentheses; labels within square brackets are relative $B(E2)$ values. Upper limits reflect limits on lifetimes and/or unknown $E2/M1$ mixing ratios δ. For clarity, the relatively enhanced or dominant transitions are shown; i.e., those with $B(E2)$ values > 1 W.u., or relative $B(E2)$ values $> 1\%$. The transition rate data for the 3064-keV, 3240-keV, and 3275-keV levels are taken from Ref. [7] and Ref. [23]. The $B(E2; 2706\text{ keV} \rightarrow 2288\text{ keV})$ value is taken from Ref. [7], and for the $B(E2; 2706\text{ keV} \rightarrow 1542\text{ keV})$ value a second solution of $0.09^{+0.056}_{-0.09}$ W.u. is possible. Combined with Fig. 9, all positive-parity states below 2.8 MeV are shown

by Sakai [65] as the 2561-keV 4^+ state, but it is assigned as a two quasiparticle state. Enhanced $E2$ transitions are observed for the $4^+ \rightarrow 2^+$ and $5^+ \rightarrow 3^+$ transitions, as well as for transitions to the ground-state band, clearly establishing the present band members. The very large limits on the transitions from the 5^+ and 6^+ states to the ground-state band arise from the unknown magnitudes of the mixing ratios δ; the present $(n, n'\gamma)$ study did not achieve the required sensitivity to enable their determination.

In Refs. [6,7], a new $K^\pi = 2^+$ band was suggested built on the intruder configuration. As mentioned above, a weak γ-ray branch corresponding to the 2706-keV $4_5^+ \rightarrow$ 2288-keV 2_4^+ transition was observed [6,7] with $B(E2; 4^+ \rightarrow 2^+) = 55 \pm 14$ W.u. – clearly an enhanced $E2$ transition. The 6^+ state at 3240 keV possesses a favoured decay to the 4^+ level at 2706 keV (the other possible favoured decay branches are mixed $E2/M1$ $I \rightarrow I$ transitions for which the mixing ratio has not been measured), strongly suggestive of a band structure.

In Refs. [6,7], the 3^+ state at 2566 keV and the 5^+ state at 3008 keV were assigned as members of the 2^+ band built on the 2288 keV state. These assignments were based on two observations; 1) the existence of a large decay branch from the 3240-keV 6^+ state to the 3008-keV 5^+ state, and 2) the existence of an enhanced transition from the 3^+ state at 2566 keV to the 2^+ intruder state at 1783 keV. However, despite the high level of sensitivity achieved in the β-decay study of ^{110}In [7], the $5^+ \rightarrow 3^+$ transition was not observed. Furthermore, no transition from the 3^+ member to the 2^+ band head was observed, nor from the 2706-keV 4^+ state to the 3^+ level. Without the observation of these latter transitions, the assignment must be taken as tentative.

3.5 Hexadecapole and $K^\pi = 4^+$ bands

Significant $E4$ strength was observed in proton and deuteron inelastic-scattering reactions with the 2220-keV 4_2^+ state the strongest one excited via a $B(E4; 4_2^+ \rightarrow 0_1^+) = 14.0(24)$ W.u. [52]. This state is a member of the $K^\pi = 2^+$ band discussed above. The observation of $E4$ strength in a $K = 2$ band is not unprecedented; for example, studies of well-deformed rare-earth nuclei [66] revealed a need for the inclusion of the Y_{42} mode in the γ band in order to explain the population of the $I, K^\pi = 4, 2^+$ state in inelastic scattering.

The 2561-keV 4_4^+ state, that appears to be strongly populated in the (d, t) transfer reaction and thus having a large contribution from the $\nu s_{1/2} \otimes g_{7/2}$ two-quasineutron configuration, has an enhanced $B(E2; 4_4^+ \rightarrow 2_2^+)$ value of 9(4) W.u. Aside from the 2220-keV 4_2^+ state, it is the only other 4^+ state that has an observed enhanced $B(E2)$ value to the $K^\pi = 2^+$ band head. It is thus a candidate for the $K^\pi = 4^+$ band head expected from the triaxial nature of the ground state [37]. In the inelastic-scattering reactions, however, it was also observed to have significant $E4$ strength with $B(E4; 4_4^+ \rightarrow 0_1^+) = 5.9(7)$ W.u. [52]. It is suggested that the collective hexadecapole excitation is fragmented amongst several states.

3.6 Isovector quadrupole excitations

A consequence of treating the protons and neutrons as separate fluids is that they can be coupled in a symmetric or anti-symmetric way [67], where the anti-symmetric coupling is often referred to as the isovector or mixed-symmetry mode [68–71]. A signature of isovector positive-parity excitations are enhanced $B(M1)$ values to low-lying positive-parity states. In well-deformed nuclei, the lowest-lying isovector mode is the 1^+_{ms} so-called scissors mode, whereas in vibrational or γ-soft nuclei it is the 2^+_{ms} mixed-symmetry state. The (γ, γ') measurements [53] identified the 1^+ state at 3044 keV in ^{110}Cd as the mixed-symmetry state that fit well with the systematics in the Cd isotopes. The identification of 2^+_{ms} candidates have remained more elusive. In ^{112}Cd, candidates were suggested [13] to have the main fragments of the 2^+_{ms} state at 2156 and 2231 keV, but later work re-interpreted these states as a member of the 0^+_4 band and the intruder $K = 2$ band head, respectively [6,7]. In the present work, the 2^+ state with the largest $B(M1; 2^+ \rightarrow 2^+_1)$ value is at 2787 keV. This state decays with a small branch to the ground state and the dominant branch (95%) to the 2^+_1 state with two possible values of the mixing ratio; $\delta = 0.204^{+0.079}_{-0.062}$ or $1.46^{+0.23}_{-0.21}$. While the larger mixing ratio cannot be excluded, it leads to a $B(E2; 2^+_8 \rightarrow 2^+_1) = 10.7(14)$ W.u. which we consider unlikely. Using the smaller result for the mixing ratio yields $B(M1; 2^+_8 \rightarrow 2^+_1) = 0.149(13)\ \mu^2_N$, making the 2787 keV state the leading candidate for the 2^+_{ms} state.

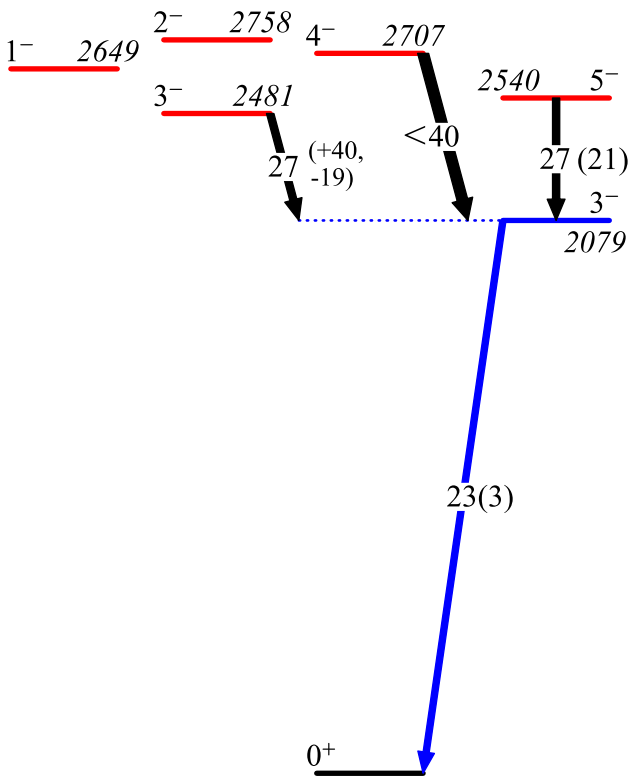

Fig. 11 Candidate levels for members of the quadrupole-octupole coupled configuration. The 3^-_1 level is a collective octupole excitation with an enhanced $B(E3; 3^-_1 \rightarrow 0^+_1) = 23(3)$ W.u. The 3^-_2 and 5^-_1 levels are shown with their $B(E2)$ values in W.u. for the transitions to the 3^-_1 level. Based on transfer results in ^{112}Cd [64], the 5^-_1 may be the rotational band member of the 3^-_1 state

3.7 Negative-parity excitations

The first 3^- state at 2079 keV can be described as a one-phonon octupole excitation due to its enhanced $B(E3)$ to the ground state of 23(3) W.u., compatible with other 3^- strengths in the region [72].

In the vibrational model, the coupling of a quadrupole excitation with an octupole excitation produces a quintuplet of negative-parity states, the quadrupole-octupole coupled states (QOC), with spins 1–5. The full quintuplet has been suggested in ^{108}Cd [73], ^{112}Cd [74,75], ^{114}Cd [76], and ^{116}Cd [77], and in ^{112,114}Cd in particular this has been supported by determinations of the absolute $B(E2)$ values that indicate considerable enhancement for decay to the 3^-_1 state – the one-phonon octupole state. In ^{110}Cd, Corminboeuf et al. [11] assigned the 5^-_1 state at 2540 keV as a member of the QOC quintuplet on the basis of its enhanced $B(E2)$ value for decay to the 3^-_1 state. However, it was recently pointed out by Jamieson et al. [64] that the 5^-_1 level in ^{112}Cd, previously assigned as the 5^- member of the QOC quintuplet [75], was dominated by the $s_{1/2} \otimes h_{11/2}$ two quasi-neutron configuration, and thus could not have the two-phonon contribution as the main one in its wave function. This reassignment was based on the fact that the 5^-_1 state was the second strongest populated state observed in the (d, p) reaction. The energy systematics of the low-lying 5^- and 6^- states are shown in Fig. 8. There is evidence from the ^{109}Ag(^{3}He, d) reaction [60] that the 5^-_1 and 5^-_2 states in ^{110}Cd at 2540 keV and 2660 keV are strongly mixed with both states having large components of the $p_{1/2} \otimes g_{9/2}$ proton configuration, and likely the $s_{1/2} \otimes h_{11/2}$ neutron configuration. The 6^- coupling of the $s_{1/2} \otimes h_{11/2}$ neutron configuration is suggested to be the 2896 keV state.

Figure 11 displays the levels that are candidates for the QOC multiplet. From the sum of the excitation energies of the 2^+_1 and 3^-_1 states, the centroid of the quintuplet is expected at 2737 keV; the observed energies range from 2481 keV to 2758 keV. The 3^-_2 and 5^-_1 states have enhanced $E2$ decays to the 3^-_1 level, although the uncertainties are substantial. From the results of Ref. [64], and the energy systematics of the 5^- states, the 5^-_1 level is more likely to be a rotational band member of the 3^- band and not a quadrupole vibration built on the octupole excitation. This interpretation was used in ^{112}Cd since it could simultaneously explain the transfer results as well as the enhanced $B(E2)$ value. The second

Table 3 Reduced electromagnetic transition rates for the levels in ^{110}Cd derived from the data in Table 1 unless otherwise noted. For $E1$ transitions, the $B(E1)$ values are calculated assuming the $M2/E1$ mixing ratio equal to 0. Values listed in square brackets are relative values. (i) denotes a state assigned as belonging to the intruder configuration

E_i(keV)	I_i^π	E_f(keV)	I_f^π	$B(E2; I_i \to I_f)$(W.u.)	$B(M1; I_i \to I_f)(\mu_N^2)$	$B(E1; I_i \to I_f)(10^{-3}$W.u.)
657.8	2_1^+	0.0	0_1^+	27.0(8)[a]		
1473.1	$0_2^+(i)$	657.8	2_1^+	< 40		
1475.8	2_2^+	657.8	2_1^+	27(2)[b]	$0.008^{+0.003b}_{-0.002}$	
		0.0	0_1^+	$0.94^{+0.06b}_{-0.04}$		
1542.4	4_1^+	657.8	2_1^+	42(9)[a]		
1731.3	0_3^+	1475.8	2_2^+	< 1680		
		657.8	2_1^+	< 7.9		
1783.6	$2_3^+(i)$	1475.8	2_2^+	< 8	< 0.02	
		1473.1	$0_2^+(i)$	29(5)		
		657.8	2_1^+	$0.32^{+0.14}_{-0.10}$	0.026(3)	
				$6.7^{+1.0}_{-0.9}$	0.0080(13)	
		0.0	0_1^+	0.28(4)		
2078.9	3_1^-	1783.6	$2_3^+(i)$			0.21(3) / 0.26(4)[c]
		1475.8	2_2^+			$0.35^{+0.05}_{-0.04}$ / $0.41^{+0.06c}_{-0.05}$
		657.8	2_1^+			0.17(2) / 0.20(3)[c]
2078.9	0_4^+	1783.6	$2_3^+(i)$	[100]		
		1475.8	2_2^+	[< 0.65]		
		657.8	2_1^+	[0.010]		
2162.8	3_1^+	1783.6	$2_3^+(i)$	< 6	< 0.0019	
		1542.5	4_1^+	$2.4^{+0.9}_{-0.8}$	0.015(5)	
				39(12)	0.008(3)	
		1475.8	2_2^+	22.7(69)	0.0073(23)	
		657.8	2_1^+	0.85(25)	0.0019(6)	
2220.1	4_2^+	1783.6	$2_3^+(i)$	< 0.5		
		1542.5	4_1^+	$10.7^{+4.9}_{-4.8}$	0.066(29)	
		1475.8	2_2^+	22(10)		
		657.8	2_1^+	0.14(6)		
2250.6	$4_3^+(i)$	1783.6	$2_3^+(i)$	115(35)		
		1542.5	4_1^+	$1.8^{+1.5}_{-1.0}$	0.119(36)	
		1475.8	2_2^+	1.2(4)		
		657.8	2_1^+	0.14(4)		
2287.5	2_4^+	657.8	2_1^+	4.78(35)	$0.0056^{+0.0009}_{-0.0008}$	
				0.0023(9)	0.033(2)	
2331.9	0_5^+	1783.6	2_3^+	6(4)		
		1475.8	2_2^+	0.9(6)		
		657.8	2_1^+	0.7(4)		
2355.8	2_5^+	1783.6	$2_3^+(i)$	< 5	< 0.004	
		1731.3	0_3^+	23.6(22)		
		1542.5	4_1^+	< 5		
		1475.1	2_2^+	$0.7^{+0.6}_{-0.5}$	$0.0026^{+0.0008}_{-0.0011}$	
		1473.1	$0_2^+(i)$	< 1.9		

Table 3 continued

E_i(keV)	I_i^π	E_f(keV)	I_f^π	$B(E2; I_i \to I_f)$(W.u.)	$B(M1; I_i \to I_f)(\mu_N^2)$	$B(E1; I_i \to I_f)(10^{-3}$W.u.)
		657.8	2_1^+	3.2(3)	$0.0027^{+0.0007}_{-0.0006}$	
				$0.009^{+0.023}_{-0.008}$	0.022(2)	
2433.2	3_2^+	2162.8	3_1^+	< 480	< 0.012	
		2078.9	3_1^-			< 0.06
		1542.5	4_1^+	< 2.3	< 0.007	
		1475.8	2_2^+	< 7	< 0.005	
		657.8	2_1^+	< 0.3	< 0.00006	
2477.4	2_6^+	2162.8	3_1^+	< 33	< 0.057	
				< 230	< 0.012	
		2078.9	$0_4^+/3_1^-$	< 130		< 0.35
		1731.3	0_3^+	< 8		
		1475.8	2_2^+	< 0.14	< 0.01	
				< 4	< 0.0007	
		1473.1	0_2^+	< 0.7		
		657.8	2_1^+	< 0.035	< 0.00002	
		0.0	0_1^+	< 0.04		
2480.0	6_1^+	2250.6	$4_3^+(i)$	$36(11)^d$		
		2220.1	4_2^+	$< 5^d$		
		1542.5	4_1^+	$62(18)^d$		
2481.5	3_2^-	2078.9	3_1^-	27^{+40}_{-19}	0.18(3)	
		1783.6	2_3^+			$0.266^{+0.038}_{-0.035}$
		1475.8	2_2^+			$0.182^{+0.026}_{-0.024}$
		657.8	2_1^+			$0.063^{+0.009}_{-0.008}$
2539.7	5_1^-	2078.9	3_1^-	27(21)		
		1542.5	4_1^+			0.027(21)
2561.3	4_4^+	1542.5	4_1^+	2.2(11)	$0.0003^{+0.0004}_{-0.0003}$	
				0.6(4)	0.004(2)	
		1475.8	2_2^+	9(4)		
		657.8	2_1^+	0.13(6)		
2566.5	3_3^+	1783.6	2_3^+	11(2)	$< 7 \times 10^{-5}$	
				0.25(2)	0.015(3)	
		1475.8	2_2^+	0.59(14)	0.014(3)	
		657.8	2_1^+	0.03(1)	0.006(1)	
2633.0	2_7^+	2078.9	3_1^-			0.54(3)
		1475.8	2_2^+	$1.9^{+0.2}_{-0.4}$	$0.0004^{+0.0010}_{-0.0004}$	
				$0.04^{+0.23}_{-0.04}$	$0.0058^{+0.0005}_{-0.0009}$	
		1473.1	0_2^+	3.2(2)		
		657.8	2_1^+	$0.27^{+0.07}_{-0.08}$	0.031(2)	
				2.4(2)	$0.0129^{+0.019}_{-0.015}$	
		0.0	0_1^+	0.010(3)		
2649.7	1_1^-	1473.1	0_2^+			0.400(23)
		0.0	0_1^+			$0.600^{+0.017}_{-0.016}$
2705.7	4_5^+	1542.5	4_1^+	31(9)	0.067(20)	
				$0.09^{+0.56}_{-0.04}$	0.16(4)	

Table 3 continued

E_i(keV)	I_i^π	E_f(keV)	I_f^π	$B(E2; I_i \to I_f)$(W.u.)	$B(M1; I_i \to I_f)(\mu_N^2)$	$B(E1; I_i \to I_f)(10^{-3}$W.u.)
2707.4	4_1^-	2162.8	3_1^+			< 0.8
		2078.9	3_1^-	< 2.3	< 0.033	
				< 40	< 0.0008	
		1542.5	4_1^+			< 0.15
2758.2	2_1^-	1783.6	2_3^+			0.15(3)
		1475.8	2_2^+			0.52(11)
		657.8	2_1^+			0.043(9)
2787.3	2_8^+	657.8	2_1^+	$0.6^{+0.5}_{-0.3}$	0.149(13)	
				10.7(14)	$0.050^{+0.012}_{-0.010}$	
		0.0	0_1^+	0.18(3)		
2842.7	5^-	1542.5	4_1^+			< 0.39
2869.3	2_9^+	1475.8	2_2^+	0.006(3)	0.015(6)	
		1473.1	0_2^+	2.8(5)		
		657.8	2_1^+	$0.11^{+0.33}_{-0.11}$	$0.086^{+0.010}_{-0.009}$	
				$6.5^{+1.2}_{-1.0}$	$0.021^{+0.008}_{-0.011}$	
		0.0	0_1^+	0.037(6)		
2926.7	5_1^+	2479.9	6_1^+	58^{+46}_{-39} [e]	$0.17^{+0.13}_{-0.11}$ [e]	
		2220.1	4_2^+	78^{+61}_{-52} [e]	$0.06^{+0.05}_{-0.04}$ [e]	
		2162.8	3_1^+	140^{+110}_{-90}		
		1542.4	4_1^+	$1.2^{+1.0}_{-0.8}$ [e]	$0.027^{+0.021}_{-0.018}$ [e]	

[a] Value from Ref. [23]
[b] Calculated using lifetime from Ref. [38]
[c] Two values are given corresponding to the 3_1^- lifetime determined before and after a correction for the doublet nature of the 1421-keV transition, see text for details
[d] Calculated using lifetime from Ref. [45]
[e] Calculated using mixing ratio from Ref. [23]

5^- state, at 2660 keV, did not have a measurable lifetime nor is a branch to the 3_1^- state observed, and thus does not appear to be a good candidate for the QOC state. Thus, no clear evidence has yet emerged for the existence of the QOC states in ^{110}Cd.

In Ref. [78], it was suggested that the large $B(M1; 3_i^- \to 3_1^-)$ values observed for nuclei near closed shells may reflect an isovector octupole character. In ^{112}Cd, the $B(M1; 3_2^- \to 3_1^-) = 0.25(8)\,\mu_N^2$ was determined which is one of the largest $B(M1)$ values observed for low-spin levels. In ^{110}Cd, we have the comparable value of $B(M1; 3_2^- \to 3_1^-) = 0.18(3)\,\mu_N^2$. However, as pointed out in Ref. [78], there may be a significant spin-flip contribution from the $g_{7/2}$ and $g_{9/2}$ protons components in the wave functions. These components are not expected within the valence shell but arise from the proton intruder configuration.

3.8 Partial dynamical symmetry comparisons

As shown in Refs. [35,36], the known experimental $B(E2)$ data for ^{110}Cd can be reconciled with the multiphonon-vibrational interpretation by invoking a partial dynamical symmetry (PDS) approach. This approach preserves the $U(5)$ symmetry for some states while strongly perturbing it for others, especially the spin 0^+ and 2^+ states. The data presented in Table 3 do not change the conclusions if the focus remains on the low-lying states. One of the consequences of the PDS approach is that the 0_2^+ and 2_4^+ states, which do not follow the normal decay patterns of the two ($n_d = 2$) and three ($n_d = 3$) phonon multiplets, are predicted to have predominantly an $n_d = 3$ and $n_d = 4$ character, respectively. The main fragments of the 0^+ $n_d = 2$ and the 2^+ $n_d = 3$ states are placed at higher excitation energies, and while they may be fragmented and distributed over several states, the $E2$ strength must still be present resulting in enhanced $B(E2)$ values to the 2_1^+ $n_d = 1$ (for the 0^+ state), and to the 2_2^+ and 4_1^+ $n_d = 2$ states. In Ref. [36], a possible candidate for a 2^+ state having a significant component with $n_d = 3$ was identified as the 2633-keV 2^+ state with $B(E2; 2^+ \to 4_1^+) = 25^{+4}_{-5}$ W.u. [23]. However, as outlined in Sect. 2.1, the 1091-keV $2^+ \to 4_1^+$ was re-assigned as the $3_3^+ \to 2_2^+$ transition, and we found no evidence for a possible $2^+ \to 4_1^+$ transition. In

fact, of the eleven confirmed or tentatively assigned 2^+ states below 3 MeV, none have an observed transition feeding the 4_1^+ level. A β-decay measurement of the ^{110}Ag ground state, which has $I^\pi = 1^+$, has recently been performed at the TRIUMF-ISAC facility. It has a much greater sensitivity to weak decay branches from excited 2^+ states than achieved in the present study, and is currently under analysis [79].

4 Summary

Data from a previous $(n, n'\gamma)$ study [10,11] of ^{110}Cd have been reanalysed seeking evidence for additional, mostly low-intensity, γ rays. A total of 58 new γ-ray transitions have been assigned, with 10 new levels observed. It is also recommended that 17 levels be removed from the evaluated list [23] of levels. Level lifetimes, transition mixing ratios, and transition branching ratios have been extracted. The revised level scheme provides important spectroscopic data supporting the Coulomb-excitation campaign aimed at determining, in a model-independent way, the shapes of states in ^{110}Cd.

While the current work has assigned a number of new γ-ray transitions, more work is still required to, firstly, confirm these placements and, secondly, obtain a higher precision on the spectroscopic data, and transition mixing ratios especially. It must be considered that the current analysis is based on γ-ray singles data, not $\gamma\gamma$ coincidences, and thus errors can be anticipated. Work towards alleviating the shortcomings using data from the β decay of ^{110}Ag and ^{110}In is currently underway.

Acknowledgements The assistance of Drs. T. Brown, F. Corminboeuf, L. Genilloud, and C.D. Hannant in the collection of the $(n, n'\gamma)$ data is gratefully acknowledged. The authors thank Prof. N. Orce for his careful reading of, and suggestions on, the manuscript. This work was supported in part by the Natural Sciences and Engineering Research Council (NSERC), Canada, and by the U.S. National Science Foundation under Grant No. PHY-2209178.

Data Availability Statement Data will be made available on reasonable request. [Author's comment: The datasets generated during and/or analysed during the current study are available from the corresponding author on reasonable request.]

Code Availability Statement This manuscript has no associated code/software. [Author's comment: Code/Software sharing not applicable to this article as no code/software was generated or analysed during the current study.]

References

1. F.K. McGowan, R.L. Robinson, P.H. Stelson, J.L.C. Ford Jr., Nucl. Phys. **66**, 97 (1965)
2. P.D. Barnes, J.R. Comfort, C.K. Bockelman, Phys. Rev. **155**, 1319 (1965)
3. J. Kern, P.E. Garrett, J. Jolie, H. Lehmann, Nucl. Phys. A **593**, 21 (1995)
4. P.E. Garrett, K.L. Green, J.L. Wood, Phys. Rev. C **78**, 044307 (2008)
5. P.E. Garrett, J.L. Wood, J. Phys. G **37**, 064028 (2010); corrigendum *ibid.*, 069701
6. P.E. Garrett, T.R. Rodríguez, A. Diaz Varela, K.L. Green, J. Bangay, A. Finlay, G.C. Ball, V. Bildstein, D.S. Cross, G.A. Demand, P. Finlay, A.B. Garnsworthy, G. Hackman, C.D. Hannant, B. Jigmeddorj, J. Jolie, W.D. Kulp, K.G. Leach, J.N. Orce, A.A. Phillips, A.J. Radich, E.T. Rand, M.A. Schumaker, C.E. Svensson, C. Sumithrarachchi, S. Triambak, N. Warr, J. Wong, J.L. Wood, S.W. Yates, Phys. Rev. Lett. **123**, 142502 (2019)
7. P.E. Garrett, T.R. Rodríguez, A. Diaz Varela, K.L. Green, J. Bangay, A. Finlay, G.C. Ball, V. Bildstein, D.S. Cross, G.A. Demand, P. Finlay, A.B. Garnsworthy, G. Hackman, C.D. Hannant, B. Jigmeddorj, J. Jolie, W.D. Kulp, K.G. Leach, J.N. Orce, A.A. Phillips, A.J. Radich, E.T. Rand, M.A. Schumaker, C.E. Svensson, C. Sumithrarachchi, S. Triambak, N. Warr, J. Wong, J.L. Wood, S.W. Yates, Phys. Rev. C **101**, 044302 (2020)
8. M. Siciliano, J.J. Valiente-Dobón, A. Goasduff, T.R. Rodríguez, D. Bazzacco, G. Benzoni, T. Braunroth, N. Cieplicka-Oryńczak, E. Clément, F.C.L. Crespi, G. de France, M. Doncel, S. Ertürk, C. Fransen, A. Gadea, G. Georgiev, A. Goldkuhle, U. Jakobsson, G. Jaworski, P.R. John, I. Kuti, A. Lemasson, H. Li, A. Lopez-Martens, T. Marchi, D. Mengoni, C. Michelagnoli, T. Mijatović, C. Müller-Gatermann, D.R. Napoli, J. Nyberg, M. Palacz, R.M. Pérez-Vidal, B. Sagyi, D. Sohler, S. Szilner, D. Testov, Phys. Rev. C **104**, 034320 (2021)
9. P.E. Garrett, M. Zielińska, E. Clément, Prog. Part. Nucl. Phys. **124**, 103931 (2022)
10. F. Corminboeuf, T.B. Brown, L. Genilloud, C.D. Hannant, J. Jolie, J. Kern, N. Warr, S.W. Yates, Phys. Rev. Lett. **84**, 4060 (2000)
11. F. Corminboeuf, T.B. Brown, L. Genilloud, C.D. Hannant, J. Jolie, J. Kern, N. Warr, S.W. Yates, Phys. Rev. C **63**, 014305 (2000)
12. H. Lehmann, P.E. Garrett, J. Jolie, C.A. McGrath, M. Yeh, S.W. Yates, Phys. Lett. B **387**, 259 (1996)
13. P.E. Garrett, H. Lehmann, C.A. McGrath, M. Yeh, S.W. Yates, Phys. Rev. C **54**, 2259 (1996)
14. P.E. Garrett, H. Lehmann, J. Jolie, C.A. McGrath, M. Yeh, S.W. Yates, Phys. Rev. C **59**, 2455 (1999)
15. P.E. Garrett, H. Lehmann, J. Jolie, C.A. McGrath, M. Yeh, W. Younes, S.W. Yates, Phys. Rev. C **64**, 024316 (2001)
16. P.E. Garrett, K.L. Green, H. Lehmann, J. Jolie, C.A. McGrath, M. Yeh, S.W. Yates, Phys. Rev. C **75**, 054310 (2007)
17. D. Bandyopadhyay, C.C. Reynolds, C. Fransen, N. Boukharouba, M.T. McEllistrem, S.W. Yates, Phys. Rev. C **67**, 034319 (2003)
18. D. Bandyopadhyay, C.C. Reynolds, S.R. Lesher, C. Fransen, N. Boukharouba, M.T. McEllistrem, S.W. Yates, Phys. Rev. C **68**, 014324 (2003)
19. D. Bandyopadhyay, S.R. Lesher, C. Fransen, N. Boukharouba, P.E. Garrett, K.L. Green, M.T. McEllistrem, S.W. Yates, Phys. Rev. C **76**, 054308 (2007)

20. M. Kadi, N. Warr, P.E. Garrett, J. Jolie, S.W. Yates, Phys. Rev. C **68**, 031306(R) (2003)
21. T. Belgya, G. Molnár, S.W. Yates, Nucl. Phys. A **607**, 43 (1996)
22. E. Sheldon, D.M. Van Patter, Rev. Mod. Phys. **38**, 143 (1966)
23. G. Gürdal, F.G. Kondev, Nucl. Data Sheets **113**, 1315 (2012)
24. J. Kern, A. Bruder, S. Drissi, V.A. Ionescu, D. Kusnezov, Nucl. Phys. A **512**, 1 (1990)
25. P.E. Garrett, J. Bangay, A. Diaz Varela, G.C. Ball, G.A. Demand, D.S. Cross, P. Finlay, A. Garnsworthy, L. Genilloud, K.L. Green, G. Hackman, C.D. Hannant, B. Jigmeddorj, J. Jolie, W.D. Kulp, K.G. Leach, J.N. Orce, A.A. Phillips, A.J. Radich, E.T. Rand, M.A. Schumaker, C.E. Svensson, C.S. Sumithrarachchi, S. Triambak, N. Warr, J. Wong, J.L. Wood, S.W. Yates, Phys. Rev. C **86**, 044304 (2012)
26. R.A. Meyer, L. Peker, Z. Phys. A **283**, 379 (1997)
27. J. Kumpulainen, R. Julin, J. Kantele, A. Passoja, W.H. Trzaska, E. Verho, J. Väärämäki, D. Cutoiu, M. Ivascu, Phys. Rev. C **45**, 640 (1992)
28. M. Délèze, S. Drissi, J. Kern, P.A. Tercier, J.-P. Vorlet, J. Rikovska, T. Otsuka, S. Judge, A. Williams, Nucl. Phys. A **551**, 269 (1993)
29. K. Heyde, P. van Isacker, M. Warquier, G. Wenes, M. Sambataro, Phys. Rev. **C25**, 3160 (1982)
30. R. Julin, J. Kantele, M. Luontama, A. Passoja, T. Poikolainen, A. Bäcklin, N.-G. Jonsson, Z. Phys. A **296**, 315 (1980)
31. C. Fahlander, A. Bäcklin, L. Hasselgren, A. Kavka, V. Mittal, L.E. Svensson, B. Varnestig, D. Cline, B. Kotlinski, H. Grein, E. Grosse, R. Kulessa, C. Michel, W. Spreng, H.J. Wollersheim, J. Stachel, Nucl. Phys. A **485**, 327 (1988)
32. R.F. Casten, J. Jolie, H.G. Börner, D.S. Brenner, N.V. Zamfir, W.-T. Chou, A. Aprahamian, Phys. Lett. **B297**, 19 (1992)
33. P.E. Garrett, J.L. Wood, S.W. Yates, Phys. Scr. **93**, 063001 (2018)
34. A. Leviatan, Prog. Part. Nucl. Phys. **66**, 93 (2011)
35. A. Leviatan, N. Gavrielov, J.E. García-Ramos, P. Van Isacker, Phys. Rev. C **98**, 031302(R) (2018)
36. N. Gavrielov, J.E. García-Ramos, P. Van Isacker, A. Leviatan, Phys. Rev. C **108**, L031305 (2023)
37. K. Wrzosek-Lipska, L. Próchniak, P.E. Garrett, S.W. Yates, J.L. Wood, P.J. Napiorkowski, T. Abraham, J.M. Allmond, F.L. Bello Garrote, H. Bidaman, V. Bildstein, C. Burbadge, M. Chiari, A. Diaz Varela, D.T. Doherty, S. Dutt, K. Hadyńska-Klęk, M. Hlebowicz, J. Iwanicki, B. Jigmeddorj, M. Kisieliński, M. Komorowska, M. Kowalczyk, R. Kumar, T. Marchlewski, M. Matejska-Minda, B. Olaizola, F. Oleszczuk, M. Palacz, E. Pasquali, E.E. Peters, M. Rocchini, E. Sahin, M. Saxena, J. Srebrny, A. Tucholski, Acta Phys. Polon. B **51**, 789 (2020)
38. I.Z. Piętka, K. Wrzosek-Lipska, P.E. Garrett, M. Zielińska, L. Próchniak, A. Nannini, M. Rocchini, T. Abraham, P. Aguilera, Z.T. Ahmed, J.M. Allmond, F. Angelini, M. Balogh, F.L. Bello Garrote, J. Benito, H. Bidaman, V. Bildstein, D. Brugnara, S. Buck, C. Burbadge, S. Carollo, J. Cederkäll, M. Chiari, R. Coleman, G. Colombi, G. Colucci, A. Diaz Varela, D.T. Doherty, S. Dutt, F. Ercolano, A. Ertoprak, R. Escudeiro, F. Galtarossa, A. Goasduff, B. Góngora-Servín, A. Gottardo, A. Gozzelino, B. Greaves, K. Hadyńska-Klęk, J. Heery, S.F. Hicks, Z. Huang, D. Hymers, A. Illana, J. Iwanicki, G. Jaworski, B. Jigmeddorj, D. Kalaydjieva, M. Kisieliński, R. Kjus, M. Komorowska, N. Kopeć, M. Kowalczyk, J. Kowalska, K.Z. Krutul-Bitowska, R. Kumar, A. Mai Quynh, N. Marchini, T. Marchlewski, K.R. Mashtakov, M. Matejska-Minda, D. Mengoni, C. Michelagnoli, P.J. Napiorkowski, D.R. Napoli, B. Olaizola, M. Palacz, S. Pannu, E. Pasquali, J. Pellumaj, E.E. Peters, R.M. Pérez-Vidal, S. Pigliapoco, E. Pilotto, F. Recchia, K. Rezynkina, E. Sahin, J. Samorajczyk-Pyśk, M. Saxena, M. Sedlák, J. Srebrny, A. Stolarz, K. Stoychev, C.E. Svensson, A. Tucholski, A. Trzcińska, S. Valbuena, J.J. Valiente-Dobón, J.L. Wood, S.W. Yates, L. Zago, I. Zanon, G. Zhang, T. Zidar, Acta Phys. Polon. Proc. Supp. **B18**, 2-A26 (2025)
39. K. Kumar, Phys. Rev. Lett. **28**, 249 (1972)
40. D. Cline, Ann. Rev. Nucl. Part. Sci. **36**, 683 (1986)
41. K.B. Winterbon, Nucl. Phys. A **246**, 293 (1975)
42. J. Kern, Nucl. Instrum. Methods **79**, 233 (1970)
43. E. Browne, J.K. Tuli, Nucl. Data Sheets **114**, 1849 (2013)
44. A. Diaz Varela, M.Sc. thesis, University of Guelph, unpublished (2013)
45. Y.N. Lobach, A.D. Efimov, A.A. Pasternak, Eur. Phys. J. A **6**, 131 (1999)
46. P.H. Stelson, F.K. McGowan, Phys. Rev. **121**, 209 (1962)
47. W.T. Milner, F.K. McGowan, P.H. Stelson, R.L. Robinson, R.O. Sayer, Nucl. Phys. A **129**, 687 (1969)
48. J. Wesseling, C.W. de Jager, H. de Vries, M.N. Harakeh, R. De Leo, M. Pignanelli, Phys. Lett. B **245**, 338 (1990)
49. E. Sheldon, V.C. Rodgers, Comp. Phys. Comm. **6**, 99 (1973)
50. E. Sheldon, D.M. Van Patter, Rev. Mod. Phys. **38**, 143 (1966)
51. M. Bertschy, S. Drissi, P.E. Garrett, J. Jolie, J. Kern, S.J. Mannanal, J.P. Vorlet, N. Warr, J. Suhonen, Phys. Rev. C **51**, 103 (1995); Erratum Phys. Rev. C **52**, 1148 (1995)
52. M. Pignanelli, N. Blasi, S. Micheletti, R. De Leo, L. LaGamba, R. Perrino, J.A. Bordewijk, M.A. Hofstee, J.M. Schippers, S.Y. van der Werf, J. Wesseling, M.N. Harakeh, Nucl. Phys. A **540**, 27 (1992)
53. C. Kohstall, D. Belic, P. von Brentano, C. Fransen, A. Gade, R.-D. Herzberg, J. Jolie, U. Kneissl, A. Linnemann, A. Nord, N. Pietralla, H.H. Pitz, M. Scheck, F. Stedile, V. Werner, S.W. Yates, Phys. Rev. C **72**, 034302 (2005)
54. N. Blasi, S. Micheletti, M. Pignanelli, R. de Leo, R. Hertenberger, M. Bisemberger, D. Hofer, H. Kader, P. Schiemenz, G. Graw, Nucl. Phys. A **536**, 1 (1992)
55. M. Pignanelli, N. Blasi, S. Micheletti, R. De Leo, M.A. Hofstee, J.M. Schippers, S.Y. van der Werf, M.N. Harakeh, Nucl. Phys. A **519**, 567 (1990)
56. V.M. Kartashov, A.I. Oborovsky, A.G. Troitskaya, Bull. Russ. Acad. Sci. Phys. **57**, 1554 (1993)
57. Y. Kawase, K. Okano, S. Uehara, T. Hayashi, Nucl. Phys. A **193**, 204 (1972)
58. A.M. Demidov, S.M. Zlitni, V.A. Kurkin, J.M. Rateb, S.M. Sergiva, A.M. Shermit, Bull. Rus. Acad. Sci. Phys. **56**, 8 (1992)
59. P.E. Garrett, E. Phys, J. Web of Conf. **66**, 02039 (2014)
60. R.L. Auble, D.J. Horen, F.E. Bertrand, J.B. Ball, Phys. Rev. C **6**, 2223 (1972)
61. J.B. Ball, C.B. Fulmer, Phys. Rev. **172**, 1199 (1968)
62. P.E. Garrett, W. Younes, J.A. Becker, L.A. Bernstein, E.M. Baum, D.P. DiPrete, R.A. Gatenby, E.L. Johnson, C.A. McGrath, S.W. Yates, M. Devlin, N. Fotiades, R.O. Nelson, B.A. Brown, Phys. Rev. C **68**, 024312 (2003)
63. S. Juutinen, R. Julin, M. Piiparinen, P. Ahonen, B. Cederwall, C. Fahlander, A. Lampinen, T. Lonnroth, A. Maj, S. Mitarai, D. Muller, J. Nyberg, P. Simecek, M. Sugawara, I. Thorslund, S. Tormanen, A. Virtanen, R. Wyss, Nucl. Phys. A **573**, 306 (1994)
64. D.S. Jamieson, P.E. Garrett, V. Bildstein, G.A. Demand, P. Finlay, K.L. Green, K.G. Leach, A.A. Phillips, C.S. Sumithrarachchi, C.E. Svensson, S. Triambak, G.C. Ball, T. Faestermann, R. Hertenberger, H.-F. Wirth, Phys. Rev. C **90**, 054312 (2014)
65. M. Sakai, Atom. Data Nucl. Data Tables **31**, 399 (1984)
66. T. Ichihara, H. Sakaguchi, M. Nakamura, M. Yosoi, M. Ieiri, Y. Takeuchi, H. Togawa, T. Tsutsumi, S. Kobayashi, Phys. Lett. B **182**, 301 (1986)
67. K. Heyde, J. Sau, Phys. Rev. C **33**, 1050 (1986)
68. A. Arima, T. Otsuka, F. Iachello, I. Talmi, Phys. Lett. B **66**, 205 (1977)
69. T. Otsuka, A. Arima, F. Iachello, Nucl. Phys. A **309**, 1 (1978)
70. F. Iachello, Phys. Rev. Lett. **53**, 1427 (1984)
71. F. Iachello, A. Arima, *The Interacting Boson Model* (Cambridge University Press, Cambridge, UK, 1987)

72. T. Kibédi, R.H. Spear, Atom. Data Nucl. Data Tables **80**, 35 (2002)
73. A. Gade, A. Fitzler, C. Fransen, J. Jolie, S. Kasemann, H. Klein, A. Linnemann, V. Werner, P. von Brentano, Phys. Rev. C **66**, 034311 (2002)
74. S. Drissi, P.A. Tercier, H.G. Börner, M. Délèze, F. Hoyler, S. Judge, J. Kern, S.J. Mannanal, G. Mouze, K. Schreckenbach, J.P. Vorlet, N. Warr, A. Williams, C. Ythier, Nucl. Phys. A **614**, 137 (1997)
75. P.E. Garrett, H. Lehmann, J. Jolie, C.A. McGrath, M. Yeh, S.W. Yates, Phys. Rev. C **59**, 2455 (1999)
76. D. Bandyopadhyay, C.C. Reynolds, S.R. Lesher, C. Fransen, N. Boukharouba, M.T. McEllistrem, S.W. Yates, Phys. Rev. C **68**, 014324 (2003)
77. J.C. Batchelder, J.L. Wood, P.E. Garrett, K.L. Green, K.P. Rykaczewski, J.-C. Bilheux, C.R. Bingham, H.K. Carter, D. Fong, R. Grzywacz, J.H. Hamilton, D.J. Hartley, J.K. Hwang, W. Krolas, W.D. Kulp, Y. Larochelle, A. Piechaczek, A.V. Ramayya, E.H. Spejewski, D.W. Stracener, M.N. Tantawy, J.A. Winger, E.F. Zganjar, Phys. Rev. C **80**, 054318 (2009)
78. M. Scheck, P.A. Butler, C. Fransen, V. Werner, S.W. Yates, Phys. Rev. C **81**, 064305 (2010)
79. S. Lange, unpublished (2025)